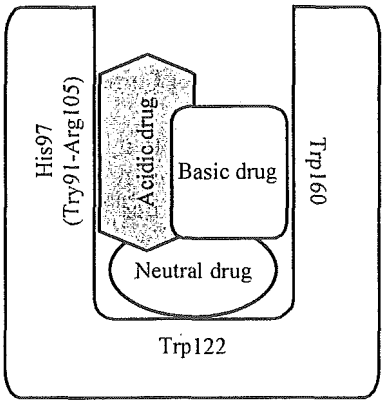

Fig. 9. Proposed drug-binding region of AGP

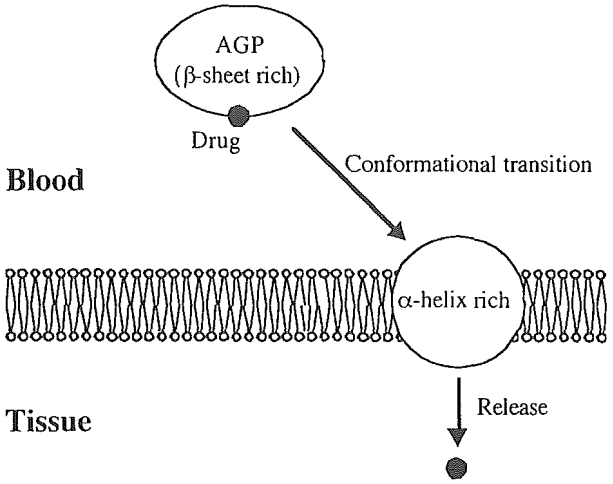

Fig. 10. Proposed mechanism for the AGP-mediated drug transport system

AGP in the native form by chromatography on an immobilized copper (II) affinity adsorbent, and determined the affinities of the two main gene products of AGP (i.e., the A variant and a mixture of the F1 and S variants) for 35 chemically diverse drugs and reported meaningful 3D-QSARs for each binding site.[92] Affinities were obtained by displacement experiments, leading to qualitative information concerning the binding sites. In particular, drugs that bind selectively to the A variant displayed some common structural features, but this was not seen for the F1*S variants. In addition, Herve *et al* found changes in the expression and microheterogeneity of the genetic variants of AGP in malignant mesothelioma.[93] This suggests that ratio of the F1*S to the A variants can vary under certain disease conditions, and that the drug-binding selectivity of variants is important factor for monitoring the AGP-binding drugs. Moreover, Jolliet-Riant *et al.* found that AGP binding decreases brain drug transfer when the A variant is mainly and almost exclusively involved in the binding.[94] On the contrary, the entire fraction of the tested drugs when bound exclusively or partly to the F1*S variant is available for transfer to the brain. This indicates the importance of understanding the drug-binding selectivity of AGP-binding drugs to variants.

AGP-mediated Drug Transport

The hypothesis that the membrane transport of a drug depends on the non-bound drug concentration is widely accepted. However, because this hypothesis does not fully explain the mechanism of uptake of some AGP-binding drugs, a protein-mediated uptake system has been proposed. In such a system, structural changes in the protein, due to interaction with the membrane surface decreases the drug-binding capacity.[95-97] Recent ESR spectroscopic findings show that the structure of HSA changes after it interacts with the surface of hepatocytes supports this proposed system.[98] It was recently reported that AGP binds to the vascular endothelial cell surface and then causes transcytosis across the cell without passing the intercellular junction.[94] Andersen detected AGP on the surface of human monocytes, granulocytes, and lymphocytes using fluorescent electron microscopy.[100,101] Maeda *et al.* found that AGP binds to the membrane surface of erythrocyte and stabilizes it.[102] Other studies of interaction of AGP with vesicles[103] and liposomes[104] also support the conclusion that AGP interacts with the membrane in circulation and may influence intracellular events.

We previously examined the structural properties and ligand-binding capacity of AGP in interactions with reverse micelles, and detailed information was obtained by comparing several different states of AGP.[105] Interaction with reverse micelles induced a unique conformational transition (β-sheet to α-helices) in AGP and decreased the binding capacity for the basic drug, chlorpromazine and the steroid hormone, progesterone to AGP. These structural conformations are very similar to those observed under conditions of acidity and high ionic strength (pH 2.0, 1.5 M NaCl). This structure seems to be an intermediate between the native state and the denatured state, possibly a molten globule. The present results suggest that, when AGP interacts with a biomembrane, it undergoes a structural transition to a unique structure that is different from both the native and denatured states and has a reduced ligand-binding capacity (**Fig. 10**). In addition, we investigated the structural properties and ligand-binding capacity of AGP under mild acidic conditions and its interactions with liposomes prepared from neutral or anionic lipids and the neutral drug, progesterone.[106] Interestingly, AGP had a unique structure at pH 4.5, at which the tertiary structure changed, whereas the secondary struc-

ture remained intact. Furthermore, the binding capacity of AGP for progesterone did not change significantly under these conditions. It was also observed that AGP was strongly bound to the anionic membrane at pH 4.5, forming an α-helix-rich structure from the original β-sheet-rich structure, which significantly decreased the binding capacity of AGP for progesterone. The structural transitions as well as the membrane binding were suppressed by adding NaCl. These results indicate that AGP has a unique structure on the membrane surface under mildly acidic conditions. The conformational change induces the molecule to bind to the membrane, aided by electrostatic interactions, and AGP subsequently assumes a predominantly α-helical conformation. Moreover, we found that alkanols, diols, and halogenols all induce such a conformational change.[107] An increase in the length and bulkiness of the hydrocarbon group and the presence of a halogen atom promoted this conversion, whereas the presence of a hydroxyl group inhibited it. Moreover, the effect was dependent on the hydrophobic and electrostatic properties of the alcohols. These results indicate that, in a membrane environment, hydrophobic and electrostatic factors cooperatively induce the transition of AGP from a β-sheet to an α-helix.

Development of Fluorescence Reagent for AGP Determination in Plasma

The human AGP level in plasma is between about 50 and 100 mg/100 mL. The AGP level can increase considerably in certain diseases, the use of drugs and in pregnancy.[9,108,109] AGP is commonly measured by a single immunodiffusion (SRID) method.

We attempted to develop a fluorescent probe that is superior to conventional ones (8-anilino-1-naphthalenesulfonate and auramine O) for use in the study of the drug-binding sites on AGP.[110] It was found that quinaldine red (QR) strongly bound to AGP and had an enhanced fluorescence in the presence of AGP at a longer wavelength, although QR was rarely fluorescent in an aqueous or albumin solution. The binding parameters of QR to AGP were K: 1.3×10^6 M^{-1} and n: 0.9, using the fluorometric titration method. The fluorescence of QR in the AGP solution, however, was markedly quenched in the presence of basic drugs, indicating that these drugs competitively displaced QR from its binding site; the results were in good agreement with those in the literature. The good relationship between binding affinities and partition coefficients suggest that hydrophobic forces are involved in the binding of basic drugs to AGP. Moreover, the polarity of the binding site of AGP, as estimated from the relationship between the emission maximum of QR and Z values was 70, which corresponds to the same Z value of acetonitrile. These results distinguish QR from other conventional AGP probes as a better fluorescent probe for developing an understanding of drug-AGP interaction and the characterization of binding sites on AGP in more detail.

AGP is an acute phase protein, the plasma level of which can be used as a diagnostic and prognostic aid during clinical therapy. This has implications for the monitoring of the free fractions of basic drugs during clinical therapy. Therefore, we examined different fluorescent probes that might be suitable for the fluorometric determination of AGP in serum.[111] Taking advantage of the enhanced fluorescence of QR in the presence of AGP, we developed a direct method for the determination of serum AGP without the need to remove other serum proteins, such as albumin. The AGP concentrations in sera of healthy volunteers and patients were correlated well with results obtained using the conventional single radial immunodiffusion (SRID) method ($r = 0.93$, slope $= 1$). The new method is faster and has a larger analytical concentration range than the SRID method. This method can also be used to determine AGP in serum for diagnosis and prognosis aid and it can serve to monitor AGP serum concentrations for the pharmacokinetic evaluation of basic drugs.

Conclusion

This review mainly summarizes recent findings including our data regarding drug-plasma protein interactions. Recent work with approaches such as the use of recombinant mutants and structural biology has proved much new information concerning the structural and functional characteristics of HSA and AGP. Advances in current DNA recombinant technologies enable the preparation of albumin and AGP with multifunctional properties. These proteins could possibly be useful as drug delivery system (DDS) carriers although the application of plasma protein to DDS has not been discussed because of space considerations. Plasma protein science including drug-binding interactions is entering a new phase of development.

Acknowledgements: The author would like to express sincere thanks to Drs. T. Maruyama, A. Suenaga, M. Anraku, K. Nishi, Graduate School of Pharmaceutical Sciences, Kumamoto University, for their valuable advice and kind consideration. He also thanks to Dr. U. Kragh-Hansen of Aarhus University and Dr. V. T. G. Chuang of Universiti Kebangsaan Malasia, for their valuable advice.

References

1) Meyer, M. C. and Guttman, D. E.: The binding of drugs by plasma proteins. *J. Pharm. Sci.*, 57: 895–918 (1967).
2) Jusco, W. J. and Gretch, M.: Plasma and tissue protein

binding of drugs in pharmacokinetics. *Drug. Metab. Rev.*, **5**: 43–140 (1976).
3) Vallner, J. J.: Binding of drugs by albumin and plasma protein. *J. Pharm. Sci.*, **66**: 447–465 (1977).
4) Sjöholm, I.: Specificity of binding sites on plasma protein: Drug protein binding (Eds. Reidenberg, M. M. and Erill, S.) Praeger Publication, Philadelphia, 1986, pp. 36–49.
5) Müller, W. E., Rick, S. and Brunner, F.: Drug binding to human alpha1-acid glycoprotein. Focus on a single binding site, Protein binding and drug transport (Eds. Tillement, J. P. and Lindenlaub), Schattauer Verlag, Stuttgart, 1986, pp. 29–44.
6) Jusco, W. J.: Pharmacokinetics in disease state changing protein binding: The effect of disease state on drug pharmacokinetics (Ed. Benet, L. Z.). *Am. Pharm. Asso., Acad. Pharm. Sci.*, Washington DC, 1976, pp. 99–123.
7) Levy, G.: Clinical implications of interindividual differences in plasma protein binding and endogenous substances: The effect of disease states on dug pharmacokinetics (Ed. Benet, L. Z.). *Am. Pharm. Asso., Acad. Pharm. Sci.*, Washington DC, 1976, pp. 137–151.
8) Kragh-Hansen, U.: Molecular aspects of ligand binding to serum albumin. *Pharmacol. Rev.*, **33**: 17–53 (1981).
9) Kremer, J. M. H., Wilting, J., and Janssen, L. H. M.: Drug binding to human alpha-1-acid glycoprotein in health and disease. *Pharmacol. Rev.*, **40**: 1–47 (1988).
10) Peters, T., Jr.: "All about Albumin: Biochemistry, Genetics, and Medical Applications," *Academic Press*, (1996).
11) Carter, D. C. and Ho, J. X.: Structure of serum albumin. *Adv. Protein Chem.*, **45**: 153–203 (1994).
12) Curry, S., Mandelkow, H., Brick, P. and Franks, N.: Crystal structure of human serum albumin complexed with fatty acid reveals an asymmetric distribution of binding sites. *Nat. Struct. Biol.*, **5**: 827–835 (1998).
13) Sudlow, G., Birkett, D. J. and Wadem, D. N.: The characterization of two specific drug binding sites on human serum albumin. *Mol. Pharmacol.*, **11**: 824–832 (1975).
14) Yamasaki, K., Maruyama, T., Kragh-Hansen U. and Otagiri, M.: Characterization of site I on human serum albumin: concept about the structure of a drug binding site. *Biochim. Biophys. Acta*, **1295**: 147–157 (1996).
15) Watanabe, H., Kragh-Hansen U., Tanase, S., Nakajou, K., Mitarai, M., Iwao, Y., Maruyama, T. and Otagiri, M.: Conformational stability and warfarin-binding properties of human serum albumin studied by recombinant mutants. *Biochem. J.*, **357**: 269–274 (2001).
16) He, X. M. and Carter, D. C.: Atomic structure and chemistry of human serum albumin. *Nature*, **358**: 209–215 (1992).
17) Watanabe, H., Tanase, S., Nakajou, K., Maruyama, T., Kragh-Hansen U. and Otagiri, M.: Role of arg-410 and tyr-411 in human serum albumin for ligand binding and esterase-like activity. *Biochem. J.*, **349**: 813–819 (2000).
18) Maruyama, T., Watanabe, H., Tanase, S., Kragh-Hansen, U., Chuang, V. T. G. and Hirono, S.: Topology analysis of site II: A major drug binding region of human serum albumin. In in: Proc. Int. Symp. on Serum Albumin and Alpha1-acid Glycoprotein (Otagiri, M., Sugiyama, Y., Testa, B. and Tillement, J. P., Eds), Tokyo Print, Kumamoto, Japan 2001, pp 45–54.
19) Bhattacharya, A. A., Curry, S. and Franks, N. P.: Binding of the general anesthetics propofol and halothane to human serum albumin. High resolution crystal structures. *J. Biol. Chem.*, **275**: 38731–38738 (2000).
20) Eckenhoff, R. G., Petersen, C. E., Ha, C. E. and Bhagavan, N. V.: Inhaled anesthetic binding sites in human serum albumin. *J. Biol. Chem.*, **275**: 30439–30444 (2000).
21) Sengupta, S., Chen, H., Togawa, T., DiBello, P. M., Majors, A. K., Budy, B., Ketterer, M. E. and Jacobsen, D. W.: Albumin thiolate anion is an intermediate in the formation of albumin-S-S-homocysteine. *J. Biol. Chem.*, **276**: 30111–30117 (2001).
22) Narazaki, R., Hamada, M., Harada, K. and Otagiri, M.: Covalent binding between bucillamine derivatives and human serum albumin. *Pharm. Res.*, **13**: 1317–1321 (1996).
23) Ivanov, A. I., Christodoulou, J., Parkinson, J. A., Barnham, K. J., Tucker, A., Woodrow, J. and Sadler, P. J.: Cisplatin binding sites on human albumin. *J. Biol. Chem.*, **273**: 14721–14730 (1998).
24) Narazaki, R., Harada, K., Sugii, A. and Otagiri, M.: Kinetic analysis of the covalent binding of captopril to human serum albumin. *J. Pharm. Sci.*, **86**: 215–219 (1997).
25) Harada, D., Naito, S., Kawauchi, Y., Ishikawa, K., Koshitani, O., Hiraoka, I. and Otagiri, M.: Determination of reduced, protein-unbound, and total concentrations of N-acetyl-L-cysteine and L-cysteine in rat plasma by postcolumn ligand substitution high-performance liquid chromatography. *Anal. Biochem.*, **290**: 251–259 (2001).
26) Keire, D. A., Mariappan, S. V., Peng, J. and Rabenstein, D. L.: Nuclear magnetic resonance studies of the binding of captopril and penicillamine by serum albumin. *Biochem. Pharmacol.*, **46**: 1059–1069 (1993).
27) Narazaki, R. and Otagiri, M.: Covalent binding of a bucillamine derivative with albumin in sera from healthy subjects and patients with various diseases. *Pharm. Res.*, **14**: 351–353 (1997).
28) Lima, J. J.: Species-dependent binding of disopyramide enantiomers. *Drug Metab. Dispos.*, **16**: 563–567 (1988).
29) Lin, J. H.: Species similarities and differences in pharmacokinetics. *Drug Metab. Dispos.*, **23**: 1008–1021 (1995).
30) Kosa, T., Maruyama, T., and Otagiri, M.: Species differences of serum albumins: I. Drug binding sites. *Pharm. Res.*, **23**: 1607–1612 (1997).
31) Matsushita, S., Isima, Y., Chuang, V. T. G.,

Watanabe, H., Tanase, S., Maruyama, T. and Otagiri, M.: Functional analysis of recombinant human serum albumin domains for pharmaceutical applications. *Pharm. Res.*, **21**: 1924–1932 (2004).
32) Kragh-Hansen, U., Chuang, V. T. G., and Otagiri, M.: Practical aspects of the ligand-binding and enzymatic properties of human serum albumin. *Biol. Pharm. Bull.*, **21**: 695–704 (2002).
33) Benet, L. Z., Spahn-Langguth, H., Iwakawa, S., Volland, C., Mizuma, T., Mayer, S., Mutschler, E. and Lin, E. T.: Predictability of the covalent binding of acidic drugs in man. *Life Sci.*, **53**: 141–146 (1993).
34) Mizuma, T., McDonagh, A. F., Lin, E. T., and Benet, L. Z.: Photoinduced covalent binding of frusemide and frusemide glucuronide to human serum albumin. *Br J Clin Pharmacol.*, **48**: 79–87 (1999).
35) Qiu, Y., Burlingame, AL. and Benet L. Z.: Mechanisms for covalent binding of benoxaprofen glucuronide to human serum albumin. Studies by tandem mass spectrometry. *Drug Metab Dispos.*, **26**: 246–256 (1998).
36) Dickinson, R. G., Baker, P. V. and King, A. R.: Studies on the reactivity of acyl glucuronides—VII. Salicyl acyl glucuronide reactivity *in vitro* and covalent binding of salicylic acid to plasma protein of humans taking aspirin. *Biochem. Pharmacol.*, **47**: 469–476 (1994).
37) Sallustio, B. C., Fairchild, B. A. and Pannall, P. R.: Interaction of human serum albumin with the electrophilic metabolite 1-O-gemfibrozil-beta-D-glucuronide. *Drug Metab. Dispos.*, **25**: 55–60 (1997).
38) Bischer, A., Zia-Amirhosseini, P., Iwaki, M., McDonagh, A. F. and Benet, L. Z.: Stereoselective binding properties of naproxen glucuronide diastereomers to proteins. *J Pharmacokinet, Biopharm.*, **23**: 379–395 (1995).
39) Sueyasu, M., Fujito, K., Shuto, H., Mizokoshi, T., Kataoka, Y. and Oishi, R.: Protein binding and the metabolism of thiamylal enantiomers *in vitro*. *Anesth. Analg.*, **91**: 736–740 (2000).
40) Mignot, I., Presle, N., Lapicque, F., Monot, C., Dropsy, R. and Netter P.: Albumin binding sites for etodolac enantiomers. *Chirality*, **8**: 271–280 (1996).
41) Rahman, M. H., Maruyama, T., Okada, T., Imai, T. and Otagiri, M.: Study of interaction of carprofen and its enantiomers with human serum albumin—II. Stereoselective site-to-site displacement of carprofen by ibuprofen. *Biochem. Pharmacol.*, **46**: 1733–1740 (1993).
42) Yamasaki, K., Rahman, M. H., Tsutsumi, Y., Maruyama, T., Ahmed, S., Kragh-Hansen, U. and Otagiri, M.: Circular dichroism simulation shows a site-II-to-site-I displacement of human serum albumin-bound diclofenac by ibuprofen. *AAPS. PharmSciTech.*, **1**: article 12 (2000).
43) Kirchner, K. A., Voelker, J. R. and Brater, D. C.: Tubular resistance to furosemide contributes to the attenuated diuretic response in nephrotic rats. *J. Am. Soc. Nephrol.*, **2**: 1201–1207 (1992).
44) Takamura, N., Shinozawa, S., Maruyama, T., Suenaga, A. and Otagiri, M.: Effects of fatty acids on serum binding between furosemide and valproic acid. *Biol. Pharm. Bull.*, **2**: 174–176 (1998).
45) Takamura, N., Maruyama, T., Chosa, E., Kawai, K., Tsutsumi, Y., Uryu, Y., Yamasaki, K., Deguchi, T. and Otagiri, M.: Bucolome, a potent binding inhibitor for furosemide, alters the pharmacokinetics and diuretic effect of furosemide: potential for use of bucolome to restore diuretic response in nephrotic syndrome. *Drug. Metab. Dispos.*, **33**: 596–602 (2005).
46) Kawai, K., Takamura, N., Nishi, R., Jinnouchi, S., Nagamachi, S., Tamura, S., Arimori, K. and Otagiri, M.: Competitive displacement of serum protein binding to regulate pharmacokinetics. In in: Proc. Int. Symp. on Serum Albumin and Alpha1-acid Glycoprotein (Otagiri, M., Sugiyama, Y., Testa, B. and Tillement, J. P., Eds), pp. 181–192 (2001).
47) Sakai, T., Maruyama, T., Sako, T., Ahmed, S., Zuidema, X., Fujiyama, S. and Otagiri, M.: Stereoselective serum protein binding of ketoprofen in liver diseases. *Enantiomer.*, **4**: 477–482 (1999).
48) Lindup, W. E., Henderson, S. J., and Barker, C. E.: Drug binding in renal disease: Plasma binding of drugs and its consequences (Eds. Belpaire, F., Borgaert, M., Tillement, J. P. and Verbekk, R.) *Academic Press*, 103–120 (1991).
49) Sakai, T., Maruyama, T., Imamura, H., Shimada, H. and Otagiri, M.: Mechanism of stereoselective serum binding of ketoprofen after hemodialysis. *J. Pharmacol. Exp. Ther.*, **278**: 786–792 (1996).
50) Ghuman, J., Zunszain, P. A., Petitpas, I., Bhattacharya, A. A., Otagiri, M. and Curry, S.; Structural basis of the drug-binding specificity of human serum albumin. *J. Mol. Biol.*, **353**: 38–52 (2005).
51) Takamura, N., Maruyama, T. and Otagiri, M.: Effects of uremic toxins and fatty acids on serum protein binding of furosemide: possible mechanism of the binding defect in uremia. *Clin. Chem.*, **43**: 2274–2280 (1997).
52) Tsutsumi, Y., Deguchi, T., Takano, M., Takadate, A., Lindup, W. E. and Otagiri, M.: Renal disposition of a furan dicarboxylic acid and other uremic toxins in the rat. *J. Pharmacol. Exp. Ther.*, **303**: 880–887 (2002).
53) Deguchi, T., Ohtsuki, S., Otagiri, M., Takanaga, H., Asaba, H., Mori, H. and Terasaki, T.: Major role of organic anion transporter 3 in the transport of indoxyl sulfate in the kidney. *Kidney Int.*, **61**: 1760–1768 (2002)
54) Deguchi, T., Kusuhara, H., Takadate, A., Endou, H., Otagiri, M. and Sugiyama, Y.: Characterization of uremic toxin transport by organic anion transporters in the kidney. *Kidney Int.*, **65**: 162–174 (2002).
55) Deguchi, T., Kouno, Y., Terasaki, T., Takadate, A. and Otagiri, M.: Differential contribution of rOat1 (Slc22a6) and rOat3 (Slc22a8) to the *in vivo* renal uptake of uremic toxins in rats. *Pharm. Res.*, **22**: 619–627 (2005).
56) Nakajou, K., Watanabe, H., Kragh-Hansen U., Maruyama, T. and Otagiri, M.: The effect of glycation on the structure, function and biological fate of human serum albumin as revealed by recombinant mutants. *Biochim. Biophys. Acta*, **1623**: 88–97 (2003).

57) Nakajou, K., Horiuchi, S., Sakai, M., Haraguchi, N., Tanaka, M., Takeya, M. and Otagiri, M.: Renal clearance of glycolaldehyde- and methylglyoxal-modified proteins in mice is mediated by mesangial cells through a class A scavenger receptor (SR-A). *Diabetologia*, **48**: 317-327 (2005).
58) Abe, T., Abe, T., Ageta, S., Kakuta, T., Suzuki, N., Hirata, H., Shouno, M., Saio, H. and Akizawa, T.: A new method for removal of albumin-binding uremic toxins: efficacy of an albumin-dialysate. *Ther. Apher.*, **5**: 58-63 (2001).
59) Mitzner, S. R., Stange, J., Klammt, S., Peszynski, P., Schmidt, R. and Noldge- Schomburg, G.: Extracorporeal detoxification using the molecular adsorbent recirculating system for critically ill patients with liver failure. *J. Am. Soc. Nephrol.*, **12**: 75-82.
60) Mitzner, S. R., Stange, J., Klammt, S., Risler, T., Erley, C. M., Bader, B. D., Berger, E. D., Lauchart, W., Peszynski, P., Freytag, J., Hickstein, H., Loock, J., Lohr, J. M., Liebe, S., Emmrich, J., Korten, G. and Schmidt, R.: Improvement of hepatorenal syndrome with extracorporeal albumin dialysis MARS: results of a prospective, randomized, controlled clinical trial. *Liver Transpl.*, **6**: 277-286 (2000).
61) Novelli, G., Rossi, M., Pretagostini, R., Poli, L., Peritore, D., Berloco, P., Di, Nicuolo, A., Iappelli, M. and Cortesini, R.: Use of MARS in the treatment of acute liver failure: preliminar monocentric experience. *Transplant. Proc.*, **33**: 1942-1944 (2001).
62) Kreymann, B., Seige, M., Schweigart, U., Kopp, K. F. and Classen, M.: Albumin dialysis: effective removal of copper in a patient with fulminant Wilson disease and successful bridging to liver transplantation: a new possibility for the elimination of protein-bound toxins. *J. Hepatol.*, **31**: 1080-1085 (1999).
63) Kawasaki, C., Nishi, R., Uekihara, S., Hayano, S. and Otagiri, M.: Charcoal hemoperfusion in the treatment of phenytoin overdose. *Am. J. Kidney Dis.*, **35**: 323-326 (2000).
64) Kawasaki, C. I., Nishi, R., Uekihara, S., Hayano, S., Kragh-Hansen U. and Otagiri, M.: How tightly can a drug be bound to a protein and still be removable by charcoal hemoperfusion in overdose cases? *Clin. Toxicol.*, **43**: 95-99 (2005).
65) Heinecke, J. W., Hsu, F. F., Crowley, J. R., Hazen, S. L., Leeuwenburgh, C., Mueller, D. M., Rasmussen, J. E. and Turk, J.: Detecting oxidative modification of biomolecules with isotope dilution mass spectrometry: Sensitive and quantitative assays for oxidized amino acids in proteins and tissues. *Methods Enzymol.*, **300**: 124-144 (1999).
66) Himmelfarb, J., McMonagle, E. and McMenamin, E.: Plasma protein thiol oxidation and carbonyl formation in chronic renal failure. *Kidney Int.* **58**: 2571-2578 (2000).
67) Sogami, M., Nagoka, S., Era, S., Honda, M. and Noguchi, K.: Resolution of human mercapt- and nonmercaptalbumin by high-performance liquid chromatography. *Int. J. Pept. Protein Res.*, **24**: 96-103 (1984).
68) Noel, J. K. and Hunter, M. J.: Bovine mercaptalbumin and non-mercaptalbumin monomers. Interconversions and structural differences. *J. Biol. Chem.*, **247**: 7391-7406 (1972).
69) Soejima, A., Kaneda, F., Manno, S., Matsuzawa, N., Kouji, H., Nagasawa, T., Era, S. and Takakuwa, Y.: Useful markers for detecting decreased serum antioxidant activity in hemodialysis patients. *Am. J. Kidney Dis.*, **39**: 1040-1046 (2002).
70) Anraku, M., Kitamura, K., Shinohara, A., Adachi, M., Suenga, A., Maruyama, T., Miyanaka, K., Miyoshi, T., Shiraishi, N., Nonoguchi, H., Otagiri, M. and Tomita, K.: Intravenous iron administration induces oxidation of serum albumin in hemodialysis patients. *Kidney Int.* **66**: 841-848 (2004).
71) Himmelfarb, J., McMenamin, E., Loseto, G. and Heinecke, J. W.: Myeloperoxidase-catalyzed 3-chlorotyrosine formation in dialysis patients. *Free Radic. Biol. Med.* **31**: 1163-1169 (2001).
72) Witko-Sarsat, V., Friedlander, M., Nguyen-Khoa, T., Capeillere-Blandin, C., Nguyen, A. T., Canteloup, S., Dayer, J. M., Jungers, P., Drueke, T. and Descamps-Latscha, B.: Advanced oxidation protein products as novel mediators of inflammation and monocyte activation in chronic renal failure. *J. Immunol.*, **161**: 2524-2532 (1998).
73) Aubert, J. P. and Loucheux-Lefebvre, M. H.: Conformational study of alpha1-acid glycoprotein. *Arch. Biochem. Biophys.*, **175**: 400-409 (1976).
74) Rojo-Dominguez, A. and Hernandez-Arana, A.: Three-dimensional modeling of the protein moiety of human alpha1-acid glycoprotein, a lipocalin-family member. *Protein Seq. Data Anal.*, **5**: 349-355 (1993).
75) Kopecky, V. Jr., Ettrich, R., Hofbauerova, K. and Baumruk, V.: Structure of human alpha1-acid glycoprotein and its high-affinity binding site. *Biochem. Biophys. Res. Commun.*, **300**: 41-46 (2003).
76) Hochepied, T., Berger, F. G., Baumann, H. and Libert, C.: Alpha1-acid glycoprotein: an acute phase protein with inflammatory and immunomodulating properties. *Cytokine Growth Factor Rev.*, **14**: 25-34 (2003).
77) Friedman, M. L., Wermeling, J. R. and Halsall, H. B.: The influence of N-acetylneuraminic acid on the properties of human orosomucoid. *Biochem. J.*, **236**: 149-153 (1986).
78) Schmid, K., Burlingame, R. W., Paulson, J. C. and Sperandio, K.: The relationship between the carbohydrate units and the secondary structure of alpha1-acid glycoprotein. *Fed. Proc.*, **37**: 1298 (1978).
79) Nishi, K., Fukunaga, N. and Otagiri, M.: Construction of expression system for human alpha1-acid glycoprotein in *Pichia pastoris* and evaluation of its drug-binding properties. *Drug Metab. Dispos.*, **32**: 1069-1074 (2004).
80) Maruyama, T., Otagiri, M. and Takadate, A.: Characterization of drug binding sites on alpha1-acid glycoprotein. *Chem. Pharm. Bull.*, **38**: 1688-1691 (1990).
81) Otagiri, M., Miyoshi, T., Yamamichi, R., Maruyama,

T. and Perrin, J. H.: Effects of tricyclic drug on induced circular dichroism spectra of dicumarol bound to alpha1-acid glycoprotein. *Biochem. Pharmacol.*, **42**: 729–733 (1991).

82) Miyoshi, T., Yamamichi, R., Maruyama, T., Takadate, A. and Otagiri, M.: Further characterization of reversal of signs of induced cotton effects of dicumarol derivatives-alpha1-acid glycoprotein systems by protriptyline. *Biochem. Pharmacol.*, **43**: 2161–2167 (1992).

83) Akinaga, S., Nomura, K., Gomi, K. and Okabe, M.: Effect of UCN-01, a selective inhibitor of protein kinase C, on the cell-cycle distribution of human epidermoid carcinoma, A431 cells. *Cancer Chemother. Pharmacol.*, **33**: 273–280 (1994).

84) Akinaga, S., Gomi, K., Morimoto, M., Tamaoki, T. and Okabe, M.: Antitumor activity of UCN-01, a selective inhibitor of protein kinase C, in murine and human tumor models. *Cancer Res.*, **51**: 4888–4892 (1991).

85) Fuse, E., Tanii, H., Takai, K., Asanome, K., Kurata, N., Kobayashi, H., Kuwabara, T., Kobayashi, S. and Sugiyama, Y.: Altered pharmacokinetics of a novel anticancer drug, UCN-01, caused by specific high affinity binding to alpha1-acid glycoprotein in humans. *Cancer Res.*, **59**: 1054–1060 (1999).

86) Fuse, E., Tanii, H., Kurata, N., Kobayashi, H., Shimada, Y., Tamura, T., Sasaki, Y., Tanigawara, Y., Lush, R. D., Headlee, D., Figg, W. D., Arbuck, S. G., Senderowicz, A. M., Sausville, E. A., Akinaga, S., Kuwabara, T. and Kobayashi, S.: Unpredicted clinical pharmacology of UCN-01 caused by specific binding to human alpha1-acid glycoprotein. *Cancer Res.*, **58**: 3248–3253 (1998).

87) Katsuki, M., Chuang, V. T., Nishi, K., Suenaga, A. and Otagiri, M.: Tryptophan residues play an important role in the extraordinarily high affinity binding interaction of UCN-01 to human alpha1-acid glycoprotein. *Pharm. Res.*, **21**: 1648–1655 (2004).

88) Katsuki, M., Chuang, V. T., Nishi, K., Kawahara, K., Nakayama, H., Yamaotsu, N., Hirono, S. and Otagiri, M.: Use of photoaffinity labeling and site-directed mutagenesis for identification of the key residue responsible for extraordinarily high affinity binding of UCN-01 in human alpha1-acid glycoprotein. *J. Biol. Chem.*, **280**: 1384–1391 (2005).

89) Chuang, V. T., Hijioka, M., Katsuki, M., Nishi, K., Hara, T., Kaneko, KI., Ueno, M., Kuniyasu, A., Nakayama, H. and Otagiri, M.: Characterization of benzodiazepine binding site on human alpha1-acid glycoprotein using flunitrazepam as a photolabeling agent. *Biochim. Biophys. Acta.*, 1725: 385–393 (2005).

90) Halsall, H. B., Austin, R. C., Dage, J. L., Sun, H. and Schlueter, K. T.: Structural aspects of alpha1-acid glycoprotein and its interaction. in: Proc. int. Symp. on Serum Albumin and Alpha1-acid Glycoprotein (Otagiri, M., Sugiyama, Y., Testa, B. and Tillement, J. P., Eds), Tokyo Print, Kumamoto, Japan. 2000, pp. 45–54.

91) Matsumoto, K., Sukimoto, K., Nishi, K., Maruyama, T., Suenaga, A. and Otagiri, M.: Characterization of ligand binding sites on the alpha1-acid glycoprotein in humans, bovines and dogs. *Drug Metab. Pharmacokinet.*, **17**: 300–306 (2002).

92) Herve, F., Caron, G., Duche, J. C., Gaillard, P., Abd Rahman, N., Tsantili-Kakoulidou, A., Carrupt, P. A., d'Athis, P., Tillement, J. P. and Testa, B.: Ligand specificity of the genetic variants of human alpha1-acid glycoprotein: generation of a three-dimensional quantitative structure-activity relationship model for drug binding to the A variant. *Mol. Pharmacol.*, **54**: 129–138 (1998).

93) Herve, F., Duche, J. C. and Jaurand, M. C.: Changes in expression and microheterogeneity of the genetic variants of human alpha1-acid glycoprotein in malignant mesothelioma. *J. Chromatogr. B Biomed. Sci. Appl.*, **715**: 111–123 (1998).

94) Jolliet-Riant, P., Boukef, M. F., Duche, J. C., Simon, N. and Tillement, J. P.: The genetic variant A of human alpha1-acid glycoprotein limits the blood to brain transfer of drugs it binds. *Life Sci.*, **62**: PL219–226 (1998).

95) Weisiger, R., Gollan, J. and Ockner, R.: Receptor for albumin on the liver cell surface may mediate uptake of fatty acids and other albumin-bound substances. *Science*, **211**: 1048–1051 (1981).

96) Forker, E. L. and Luxon, B. A.: Albumin helps mediate removal of taurocholate by rat liver. *J. Clin. Invest.*, **67**: 1517–1522 (1981).

97) Forker, E. L. and Luxon, B. A.: Albumin-mediated transport of rose bengal by perfused rat liver. Kinetics of the reaction at the cell surface. *J. Clin. Invest.*, **72**: 1764–1771 (1983).

98) Horie, T., Mizuma, T., Kasai, S. and Awazu, S.: Conformational change in plasma albumin due to interaction with isolated rat hepatocyte. *Am. J. Physiol.*, **254**: G465–470 (1988).

99) Predescu, D., Predescu, S., McQuistan, T. and Palade, G. E.: Transcytosis of alpha1-acidic glycoprotein in the continuous microvascular endothelium. *Proc. Natl. Acad. Sci. U.S.A.*, **95**: 6175–6180 (1998).

100) Andersen, M. M.: Leucocyte-associated plasma proteins. Association of prealbumin, albumin, orosomucoid, alpha1-antitrypsin, transferrin and haptoglobin with human lymphocytes, monocytes, granulocytes and a promyelocytic leukaemic cell line (HL-60). *Scand. J. Clin. Lab. Invest.*, **43**: 49–59 (1983).

101) Andersen, M. M.: Leucocyte-associated plasma proteins in leucocytes during disease states, and in leukaemic cells, *Scand. J. Clin. Lab. Invest.* **44**, 257–265 (1984).

102) Maeda, H., Morinaga, T., Mori, I. and Nishi, K.: Further characterization of the effects of alpha1-acid glycoprotein on the passage of human erythrocytes through micropores. *Cell Struct. Funct.*, **9**: 279–290 (1984).

103) Cheresh, D. A., Haynes, D. H. and Distasio, J. A.: Interaction of an acute phase reactant, alpha1-acid glycoprotein (orosomucoid), with the lymphoid cell surface: a model for non-specific immune suppression. *Immunology*, **51**: 541–548 (1984).

104) Neitchev, V. Z., and Bideaud, F. A.: Temperature-dependent osmotic permeability in glycoprotein containing liposomes. *Mol. Biol. Rep.*, **13**: 85–88 (1988).
105) Nishi, K., Sakai, N., Komine, Y., Maruyama, T., Halsall, H. B. and Otagiri, M.: Structural and drug-binding properties of alpha1-acid glycoprotein in reverse micelles. *Biochim. Biophys. Acta*, **1601**: 185–191 (2002).
106) Nishi, K., Maruyama, T., Halsall, H. B., Handa, T. and Otagiri, M.: Binding of alpha1-acid glycoprotein to membrane results in a unique structural change and ligand release. *Biochemistry*, **43**: 10513–10519 (2004).
107) Nishi, K., Komine, Y., Sakai, N., Maruyama, T. and Otagiri, M.: Cooperative effect of hydrophobic and electrostatic forces on alcohol-induced alpha-helix formation of alpha1-acid glycoprotein. *FEBS Lett.*, **579**: 3596–3600 (2005).
108) Bacchus, H.: Serum seromucoid and acid mucopolysaccharide in malignant neoplastic diseases. *Cancer*, **18**: 1285–1291 (1965).
109) Martyn, J. A., Abernethy, D. R. and Greenblatt, D. J.: Plasma protein binding of drugs after severe burn injury. *Clin. Pharmacol. Ther.*, **35**: 535–539 (1984).
110) Imamura, H., Maruyama, T. and Otagiri, M.: Evaluation of quinaldine red as a fluorescent probe for studies of drug-alpha1-acid glycoprotein interaction. *Biol. Pharm. Bull.*, **16**: 926–929 (1993).
111) Imamura, H., Maruyama, T., Okabe, H., Shimada, H. and Otagiri, M.: A simple and rapid fluorometric determination method of alpha1-acid glycoprotein in serum using quinaldine red. *Pharm. Res.*, **11**: 566–570 (1994).

0090-9556/05/3312-1911–1919$20.00
DRUG METABOLISM AND DISPOSITION
Copyright © 2005 by The American Society for Pharmacology and Experimental Therapeutics
DMD 33:1911–1919, 2005

Vol. 33, No. 12
6163/3066736
Printed in U.S.A.

HYDROLYSIS OF ANGIOTENSIN II RECEPTOR BLOCKER PRODRUG OLMESARTAN MEDOXOMIL BY HUMAN SERUM ALBUMIN AND IDENTIFICATION OF ITS CATALYTIC ACTIVE SITES

Shen-Feng Ma, Makoto Anraku, Yasunori Iwao, Keishi Yamasaki, Ulrich Kragh-Hansen, Noriyuki Yamaotsu, Shuichi Hirono, Toshihiko Ikeda, and Masaki Otagiri

Graduate School of Pharmaceutical Sciences, Kumamoto University, Kumamoto, Japan (S.-F.M., M.A., Y.I., M.O.); Department of Pharmacy, Miyazaki Medical College Hospital, Miyazaki, Japan (K.Y.); Department of Medical Biochemistry, University of Aarhus, Aarhus, Denmark (U.K.-H.); the School of Pharmaceutical Sciences, Kitasato University, Tokyo, Japan (N.Y., S.H.); and Drug Metabolism and Pharmacokinetics Research Laboratories, Sankyo Co., Ltd., Tokyo, Japan (T.I.)

Received June 21, 2005; accepted August 26, 2005

ABSTRACT:

In the present study, we investigated the esterase-like activity of human serum albumin (HSA) and the mechanism by which it hydrolyzes, and thereby activates, olmesartan medoxomil (CS-866), a novel angiotensin II receptor antagonist. CS-866 has previously been shown to be rapidly hydrolyzed in serum in which HSA appeared to play the most important role in catalyzing the hydrolysis. We found that the hydrolysis of CS-866 by HSA followed Michaelis-Menten kinetics. Compared with the release of *p*-nitrophenol from *p*-nitrophenyl acetate (PNPA), CS-866 showed lower affinity to HSA and a lower catalytic rate of hydrolysis. Thermodynamic data indicated that PNPA has a smaller value of activation entropy (ΔS) than CS-866; consequently, PNPA is more reactive than CS-866. Ibuprofen and warfarin acted as competitive inhibitors of hydrolysis of CS-866, whereas dansyl-L-asparagine, *n*-butyl *p*-aminobenzoate, and diazepam did not. These findings suggest that the hydrolytic activity is associated to parts of site I and site II for ligand binding. All chemically modified HSA derivatives (Tyr-, Lys-, His-, and Trp-modifications) had significantly lower reactivity than native HSA; Lys-HSA and Trp-HSA had especially low reactivity. All the mutant HSAs tested (K199A, W214A, and Y411A) exhibited a significant decrease in reactivity, suggesting that Lys-199, Trp-214, and Tyr-411 play important roles in the hydrolysis. Results obtained using a computer docking model are in agreement with the experimental results, and strongly support the hypotheses that we derived from the experiments.

Ester prodrugs are hydrolyzed to their pharmacologically active metabolites after absorption. Esterases present in the small intestine, plasma, and liver are involved in this process. In most cases, intestinal esterases serve as the major enzymes in activation of prodrugs during the first pass through the gut after absorption. However, prodrugs that are relatively resistant to hydrolysis by intestinal esterases enter the blood circulation and are activated by serum (plasma) and liver esterases. The major hydrolyzing enzymes in serum are cholinesterase, arylesterase, carboxylesterase, and albumin. The relative importance of each serum esterase in prodrug activation varies among animal species and prodrugs.

Olmesartan medoxomil [CS-866: (5-methyl-2-oxo-1,3-dioxolen-4-yl) methoxy-4-(1-hydroxyl-1-methylethyl)-2-propyl-1-{4-[2-(tetrazol-5-yl)-phenyl]phenyl}methylimi-dazol-5-carboxylate] is a novel nonpeptide angiotensin II receptor antagonist that acts as an antihypertensive prodrug (Koike et al., 2001; Neutel, 2001; Brousil and Burke, 2003). After oral administration, CS-866 is rapidly de-esterified, producing an active acid metabolite, olmesartan (RNH-6270) (Fig. 1) (Koike et al., 2001; Neutel, 2001; Brousil and Burke, 2003). Hydrolysis of CS-866 in serum has been observed in several species, and comparison among five species has shown that hydrolytic activity is highest in rabbits, followed by dogs, mice, rats, and humans (Ikeda, 2000). Furthermore, it was found that differences in hydrolytic activity due to serum albumin are large compared to the combined activity of all serum components. Thus, HSA might make an important contribution to activation of CS-866 after oral administration.

In the present study, we examined the esterase-like activity of HSA and the mechanism of its hydrolysis of CS-866. First, the general properties of the hydrolytic reaction of HSA with CS-866 were determined, including the kinetics and thermodynamics, and compared with those of the hydrolytic reaction between HSA and *p*-nitrophenyl acetate (PNPA) (Means and Bender, 1975; Sakurai et al., 2004). Second, to characterize the effects of exogenous compounds on hydrolysis, we investigated changes in hydrolytic activity in the

This work was supported in part by a Grant-in-Aid for Scientific Research from the Ministry of Education, Science and Culture of Japan (11694298 for M.O.) and was also supported in part by Grant-in-Aid for Scientific Research, Encouragement of Young Scientists (B) (13771414 for N.Y.) from Japan Society for the Promotion of Science.

Article, publication date, and citation information can be found at http://dmd.aspetjournals.org.

doi:10.1124/dmd.105.006163.

ABBREVIATIONS: *CS-866, olmesartan medoxomil* [(5-methyl-2-oxo-1,3-dioxolen-4-yl) methoxy-4-(1-hydroxyl-1-methylethyl)-2-propyl-1-{4-[2-(tetrazol-5-yl)-phenyl]phenyl}methylimi-dazol-5-carboxylate]; RNH-6270, olmesartan; PNPA, *p*-nitrophenyl acetate; HSA, human serum albumin; rHSA, recombinant HSA; *n*-butyl *p*-AB, *n*-butyl-*p*-aminobenzoate; DNSA, dansyl-L-asparagine; ΔG_T, free energy differences; ΔG_S, free energy change for the initial reaction of albumin and substrate; ΔG, activation free energy; ΔH, activation enthalpy change; ΔS, activation entropy change.

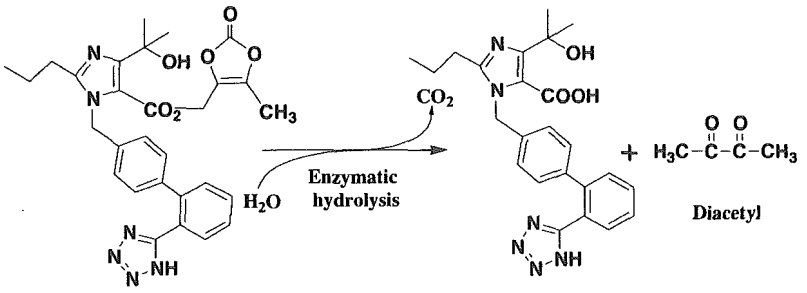

Olmesartan medoxomil CS-866
Ester prodrug

Olmesartan RNH-6270
Active metabolite

FIG. 1. Hydrolysis of CS-866 to RNH-6270

presence and absence of various ligands. Then, we examined the importance of certain types of amino acid residues of HSA for the hydrolysis of CS-866, using chemical modification techniques. Recombinant HSA (rHSA) proteins with alterations of specific amino acid residues were prepared using site-directed mutagenesis techniques, to obtain detailed information about the contribution of those residues. Finally, computer docking models of CS-866 and HSA were constructed and were found to be consistent with the experimental results.

Materials and Methods

Materials. HSA was donated by the Chemo-Sera-Therapeutic Research Institute (Kumamoto, Japan). HSA was defatted before use (Chen, 1967).

CS-866 and RNH-6270 were donated by Sankyo Co., Ltd. (Tokyo, Japan). PNPA, succinic anhydride and *n*-butyl *p*-aminobenzoate (*n*-butyl *p*-AB) were purchased form Nakalai Tesque (Kyoto, Japan). Warfarin was obtained from Eisai Co. (Tokyo, Japan), ibuprofen was obtained from Kaken Pharmaceutical Co. (Osaka, Japan), diazepam was obtained from Sumitomo Pharmaceutical Co. (Osaka, Japan), tetranitromethane was obtained from Aldrich Chemical Co. (Milwaukee, WI), and trinitrobenzenesulfonic acid was obtained from Wako Pure Chemical Industries, Ltd. (Osaka, Japan). Dansyl-L-asparagine (DNSA), 2-hydroxyl-5-nitrobenzyl bromide, and diethyl pyrocarbonate were purchased from Sigma-Aldrich (St. Louis, MO). Restriction enzymes, T4 polynucleotide kinase, calf intestinal alkaline phosphatase, a DNA ligation kit, TaKaRa EX *Taq*DNA polymerase, and a site-directed mutagenesis kit (oligonucleotide-directed dual amber method) were obtained from Takara Shuzo Co., Ltd. (Kyoto, Japan). A DNA sequence kit was obtained from Applied Biosystems (Tokyo, Japan). The *Pichia* Expression kit was purchased from Invitrogen (Carlsbad, CA). All other chemicals were of analytical grade.

Esterase-Like Activity Measurement. *Procedures for Michaelis-Menten Equation Runs.* The reaction was started by adding CS-866 in 100% acetonitrile (5 μl) to preincubated HSA (120 μl, 75 μM), at a final concentration of 10 to 250 μM. Incubation proceeded for 10 min and was terminated by adding 500 μl of acetonitrile to the incubation mixture. We have checked that 4% acetonitrile has little effect on the reaction. After centrifugation for 1 min, a 30-μl aliquot of the deproteinized supernatant was subjected to high-performance liquid chromatography, and RNH-6270 was separated from CS-866 on an ODS column using the following conditions: column, YMC-Pack ODS-AM, AM-302, 150 × 4.6 mm i.d.; column temperature, 40°C maintained by a Hitachi 655A-52 column oven; a Hitachi L-6000 pump; a Hitachi FL detector L-7480 fluorescent monitor; a HITACHI D-2500 Chromato-Integrator; mobile phase, acetonitrile/water/acetic acid, 40:60:0.1; wavelength, excitation = 260 nm, emission = 370 nm; flow rate, 1.0 ml/min.

The reaction between CS-866 and HSA took place at 4°C. Under that condition, Michaelis-Menten equation analysis can be applied.

$$v = \frac{V_{max}[S]}{K_M + [S]} \quad (1)$$

Here, [*S*] is the concentration of substrate. That is the case, because previous studies have revealed a linear relationship between 1/*V* and 1/*S* when plotted in a Lineweaver-Burk plot (Koike et al., 2001):

$$\frac{1}{v} = \frac{1}{V_{max}} + \frac{K_M}{V_{max}[S]} \quad (2)$$

Procedures for Kinetic Runs. Hydrolysis of CS-866 (5 μM) by HSA (at least a 5-fold excess concentration over the substrate) was performed using conditions able to avoid complications due to multiple reactive sites of albumin. Under such conditions, pseudofirst-order rate constant analysis can be performed. The pseudofirst-order rate constant for the release of RNH-6270 (k_{obs}), the dissociation constant of the substrate-HSA complex (K_S), and the catalytic rate constants (k_{cat}) were calculated as reported elsewhere (Sakurai et al., 2004).

Thermodynamic Analysis. Thermodynamic analysis of the HSA-catalyzed reaction was performed at temperatures ranging from 20°C to 40°C. We calculated the thermodynamic parameters, the free energy change for the initial reaction between enzyme and substrate (ΔG_S), the activation free energy for the rate-determining step (ΔG), the free energy difference for the reaction (ΔG_T), the activation energy (E_a), the activation enthalpy change (ΔH), and the activation entropy change (ΔS), using previously published methods (Sakurai et al., 2004).

Effects of Ligands. HSA (120 μl, 75 μM) was preincubated, and the enzymatic reaction was started by adding CS-866 in 100% acetonitrile (5 μl) to the solution, at a final concentration of 100 to 250 μM, in the presence or absence of each ligand (at a final concentration of 0–600 μM) (Ikeda, 2000). Incubation proceeded for 10 min at 37°C, and the release of RNH-6270 was measured by high-performance liquid chromatography as described above.

Chemical Modification of HSA. *Histidine Residues.* Chemical modification of His residues was performed using diethyl pyrocarbonate (Roosemont, 1978). An average of 2.22 His residues was modified out of the total of 16 His residues.

Lysine Residues. Chemical modification of Lys residues was performed according to the method of Gounaris and Perlmann (1967). The modification ratio was calculated as described by Haynes et al. (1967). An average of 3.80 of the 59 Lys residues was modified.

Tyrosine Residues. Chemical modification of Tyr residues was performed as outlined by Sokolovsky et al. (1966). An average of 1.24 of the 18 Tyr residues was modified.

Tryptophan Residues. Chemical modification of the single Trp residue was performed at room temperature (Fehske et al., 1978). An average of 0.88 of the 1 Trp residue was modified.

Chemical modifications of specific amino acid residues (Tyr, Lys, His, and Trp) were performed with the assumption that the effects on other amino acid residues would be negligible. The secondary and tertiary protein structures of all the modified HSAs were examined by circular dichroism measurements before use, and no significant difference was observed between the derivatives and native HSA (data not shown).

Synthesis and Purification of rHSA Forms. The recombinant DNA techniques used to produce wild-type rHSA and the single-residue mutants were

essentially the same as those described by Watanabe et al. (2001). A chimeric plasmid (pJDB-ADH-L10-HSA-A) containing cDNA for the mature form of HSA and an L10 leader sequence was donated by Tonen Co. (Tokyo, Japan). The mutagenic primers used (underlined letters indicate mismatches) were as follows: 5′-CAAACAGAGACTCGCCTGTGCCAGTCTCC-3′ for K199A; 5′-GAGCTTTCAAAGCAGCTGCAGTAGCTCGCCTG-3′ for W214A; 5′-CTATTAGTTCGTGCCACCAAG-3′ for Y411A.

The L10-HSA coding region was amplified by polymerase chain reaction using a forward and a reverse primer containing a 5′-terminal EcoRI site, and was cloned into the EcoRI-digested pKF19k vector (Takara Shuzo Co. Ltd.), and mutagenesis was then performed. The mutation was confirmed by DNA sequencing of the entire HSA coding region using the dideoxy chain termination method and an Applied Biosystems ABI Prism 310 Genetic Analyzer. To construct the HSA expression vector pHIL-D2-HSA, an L10-HSA coding region with or without the desired mutation site was incorporated into the methanol-inducible pHIL-D2 vector (Invitrogen). The resulting vector was introduced into the yeast species *Pichia pastoris* (strain GS115) to express rHSA. Secreted rHSA was isolated from the growth medium by precipitation with 60% ammonium sulfate at room temperature, and was then purified using a column of Blue Sepharose CL-6B (GE Healthcare, Little Chalfant, Buckinghamshire, UK). The eluted rHSA was deionized and then defatted using charcoal treatment.

The resulting protein exhibited a single band on an SDS/polyacrylamide gel, and all of the recombinant proteins migrated to the same position as native HSA (data not shown). Any secondary or tertiary structural differences between native (wild-type) and mutant rHSAs were analyzed by circular dichroism (data not shown). In the far-UV and near-UV regions, all rHSAs exhibited the same characteristics as native HSA.

Docking of CS-866 to HSA. To dock CS-866 to HSA, we used the crystal structure of the HSA-myristate-*S*-warfarin complex (PDB ID 1H9Z; Petitpas et al., 2001). The docking calculation of CS-866 to HSA was performed using SYBYL FlexX (Rarey et al., 1996). CS-866 docked at site I and site II. The residues within 5 Å from *S*-warfarin were defined as site I, and the residues within 5 Å from myristate-3 and -4 were defined as site II. During the docking calculation, the structure of HSA was kept rigid. The docking algorithm generated 275 and 209 different placements of CS-866 in site I and site II, respectively. All placements were evaluated using the scoring function of FlexX. For each site, because the top 10 placements exhibited nearly identical binding modes, we chose the placement with the best value as the candidate binding mode.

Refinement of Docking Models. To refine the docking models, the coordinates of CS-866 and the residues within 10 Å from CS-866 were optimized to reduce the root mean square of the gradients of potential energy to below 0.05 kcal mol^{-1} $Å^{-1}$ using SYBYL 6.9.1 (Tripos, Inc., St. Louis, MO, 2003). The Tripos force field was used for the molecular energy calculation. The AMBER 7 charges (Cornell et al., 1995) were used as the atomic charges for HSA. The Gasteiger-Hückel charges (Purcel and Singer, 1967; Gasteiger and Marsili, 1980; Marsili and Gasteiger, 1980, 1981) were used as the charges for CS-866. The cut-off distance for the nonbonded interactions was 10 Å. The distance-dependent dielectric constant of $4r$ was used. Due to the lack of the 1st and 2nd N-terminal residues and the lack of the 585th C-terminal residue in the crystal structure of HSA, the 3rd and 584th residues were protected by an acetyl group and by an *N*-methyl group, respectively. The initial positions of the other missing atoms in the crystal structure were generated by SYBYL.

Statistics. Where possible, statistical analyses were performed using Student's *t* test.

Results

Hydrolytic Kinetics. First, we were able to confirm that the hydrolysis of CS-866 by HSA followed Michaelis-Menten kinetics (data not shown). Table 1 shows the K_M, V_{max}, k_{cat}, and specificity constant (k_{cat}/K_M) values for the hydrolytic reaction.

To elucidate the reactivity of CS-866, we compared the kinetic parameters for CS-866 with those determined for the release of *p*-nitrophenol from PNPA (Table 2) (Means and Bender, 1975; Sakurai et al., 2004). The K_S value was found to be lower for CS-866, suggesting that PNPA has greater affinity than CS-866 for HSA (Fersht, 1998; Sakurai et al., 2004). The catalytic rate constant, k_{cat}, was also found to be greater for PNPA.

TABLE 1

Kinetic parameters for the hydrolytic reaction between CS-866 and HSA at pH 7.4 and 37°C

HSA Type	K_M	V_{max}	k_{cat}	k_{cat}/K_M
	μM	$nmol \cdot min^{-1}$	min^{-1}	$\mu M^{-1} \cdot min^{-1}$
Native	48.2	1.02	0.113	0.00232

[a] Reaction conditions: 75 μM HSA, 10 to 250 μM CS-866, 1/15 M phosphate buffer (pH 7.4), 37°C.

TABLE 2

Kinetic parameters for the hydrolysis of CS-866 and PNPA by HSA at pH 7.4 and 25°C

Substrate	k_{cat}	K_S	k_{cat}/K_S
	$10^{-3} \cdot s^{-1}$	μM	$M^{-1} \cdot s^{-1}$
CS-866	0.845	42.5	19.9
PNPA	86.8	217	403.4

[a] PNPA data from Sakurai et al. (2004).

TABLE 3

Thermodynamic parameters for the hydrolysis of CS-866 and PNPA by HSA

Substrate	ΔG_T	ΔG_S	ΔG	ΔH	ΔS
	$kJ \cdot mol^{-1}$	$kJ \cdot mol^{-1}$	$kJ \cdot mol^{-1}$	$kJ \cdot mol^{-1}$	$kJ \cdot mol^{-1} \cdot K^{-1}$
CS-866	71.3	−25.0	96.3	34.7	−0.207
PNPA[a]	58.1	−20.9	79.0	66.1	−0.0435

[a] PNPA data from Sakurai et al. (2004). Reaction conditions: 1/15 M phosphate buffer (pH 7.4), 25°C.

Thermodynamics. The relationship between the catalytic rate constants and temperature followed the Arrhenius equation. Accordingly, a linear relationship was found between ln k_{cat} and $1/T$, where T is the absolute temperature in degrees Kelvin (data not shown). The activation energy of the reaction, E_a, calculated from the Arrhenius plot (Fersht, 1998; Sakurai et al., 2004), was found to be 37.1 kJ · mol^{-1}.

Using the HSA-hydrolysis parameters, we compared energy changes and thermodynamic parameters between CS-866 and PNPA (Table 3). CS-866 had larger values of ΔG (96.3 kJ · mol^{-1}) and ΔS (−0.207 kJ · mol^{-1} · K^{-1}) than PNPA.

Effects of Ligands on Hydrolysis. The site I-specific ligands warfarin, DNSA, and *n*-butyl *p*-AB were used as inhibitors to investigate for any competition with the hydrolytic reaction (Yamasaki et al., 1996; Kragh-Hansen et al., 2002). Interestingly, warfarin inhibited hydrolysis in a competitive manner, with a K_i value of 155 μM in a Dixon plot (Fig. 2A). By contrast, neither *n*-butyl *p*-AB nor DNSA inhibited HSA-catalyzed hydrolysis of CS-866 (Fig. 2, B and C).

The site II-specific ligands ibuprofen and diazepam were used to investigate, whether there is competition between that ligand-binding site and the catalytic site (Kragh-Hansen et al., 2002). Diazepam had no inhibitory effect, but competitive inhibition was observed with ibuprofen, with a K_i value of 235 μM in a Dixon plot (Fig. 3A and 3B).

Effect of Chemical Modification on Hydrolysis. Hydrolytic activities of the four specifically modified HSA derivatives (Tyr-, Lys-, His-, and Trp-HSA) were assayed (Fig. 4). Compared with native-type HSA, all modified HSA derivatives had significantly decreased hydrolytic activity ($p < 0.05$). Modification of Lys residues or of the single Trp residue resulted in the most pronounced reductions in catalytic reactivity.

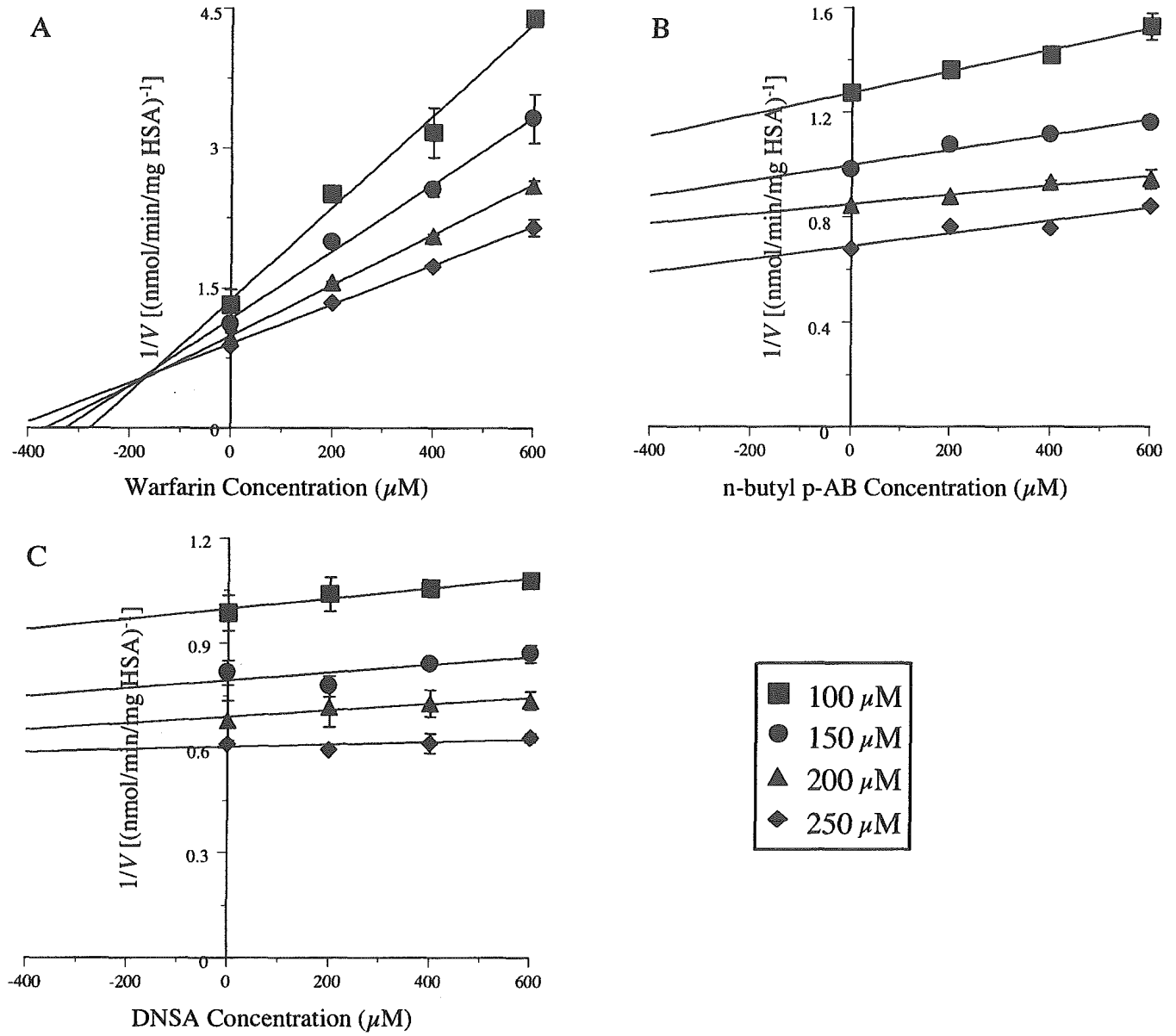

FIG. 2. Effect of warfarin (A), *n*-butyl *p*-AB (B), and DNSA (C) (0~600 μM) on the hydrolysis of CS-866 by HSA. Reaction conditions: 75 μM HSA, 100 to 250 μM CS-866, 1/15 M phosphate buffer (pH 7.4), 37°C. Plots represent mean ± S.D. (n = 3).

Examination of Hydrolytic Activity Using Site-Directed Mutagenesis. Wild-type rHSA and the HSA single-residue mutants K199A, W214A, and Y411A were used to examine involvement of various amino acid residues in the hydrolysis. The hydrolytic activity of each rHSA was examined to elucidate the contribution of specific amino acid residues (Fig. 5). Compared with the wild-type rHSA, all mutant rHSAs showed significant decreases in catalytic activity. K199A exhibited a particularly marked decrease in catalytic activity ($p < 0.01$), suggesting that Lys-199 plays a particularly important role in the hydrolysis. These results are in good agreement with those obtained with the chemically modified HSAs. The W214A and Y411A mutants showed a significant reduction in catalytic activity ($p < 0.05$), indicating that the amino acid residues Trp-214 and Tyr-411 are also involved in the hydrolytic reaction.

Molecular Interaction of CS-866 and HSA in Docking Models. We obtained two docking models: model I for site I, and model II for site II. In model I, the binding of CS-866 was similar to that of warfarin (Fig. 6). The biphenyl moiety of CS-866 was bound to the hydrophobic pocket consisting of Leu-219, Leu-238, Val-241, Leu-260, Ala-261, Ile-264, Ile-290, and Ala-291. The 2-propyl-imidazole moiety and the propan-2-ol moiety were bound to the other hydrophobic pocket (Phe-211, Trp-214, Ala-215, Leu-219, and Leu-238). Hydrogen bonds to and electrostatic interactions with other residues are detailed in Table 4. Oxygen atoms of the vinylene carbonate moiety formed hydrogen bonds with side chains of Arg-218 and of Arg-222. Negative charges of the tetrazole moiety interacted electrostatically with side chains of Lys-199 and of Arg-257. The hydroxyl oxygen atom of the propan-2-ol moiety formed a hydrogen bond with the side chain of Lys-199, and the hydrogen atom formed a hydrogen bond with the side chain of His-242. The carbonyl oxygen atom of the ester moiety formed a hydrogen bond with the side chain of Lys-199. The ester moiety of CS-866 was in the vicinity of Glu-292. However, the side chain of Glu-292 was distant from the carbonyl carbon of the ester moiety, because the docking program, FlexX, cannot account for chemical reactions and remains rigid. We changed the torsion angles

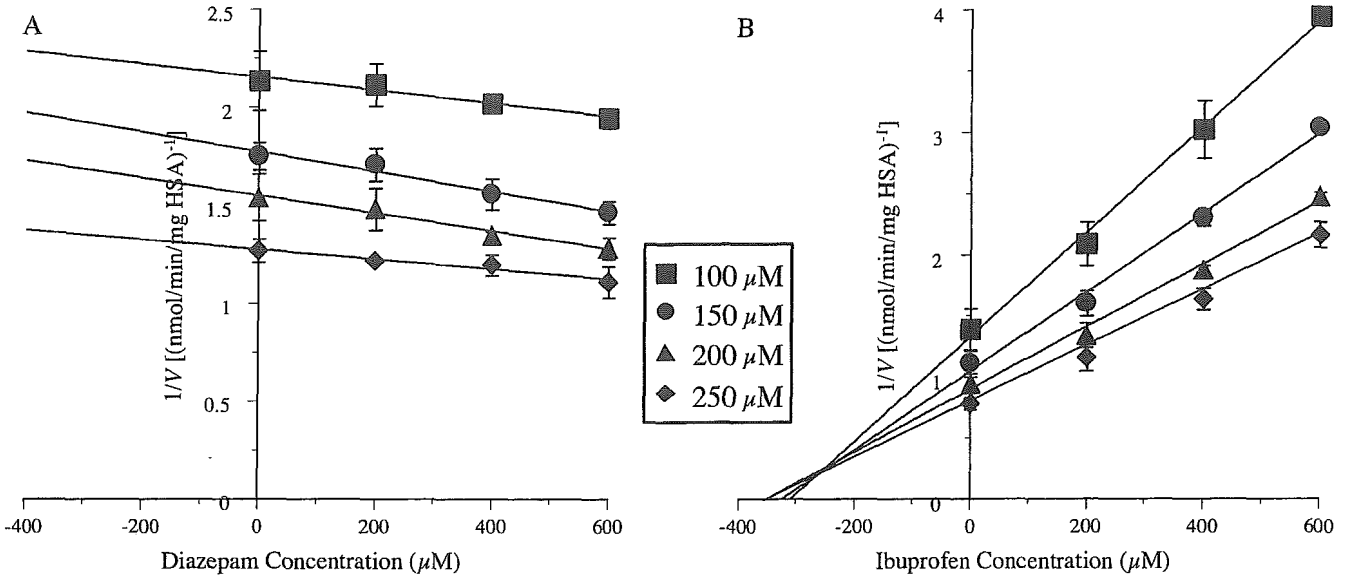

FIG. 3. Effect of diazepam (A) and ibuprofen (B) (0~600 μM) on the hydrolysis of CS-866 by HSA. Reaction conditions: 75 μM HSA, 100 to 250 μM CS-866, 1/15 M phosphate buffer (pH 7.4), 37°C. Plots represent mean ± S.D. (n = 3).

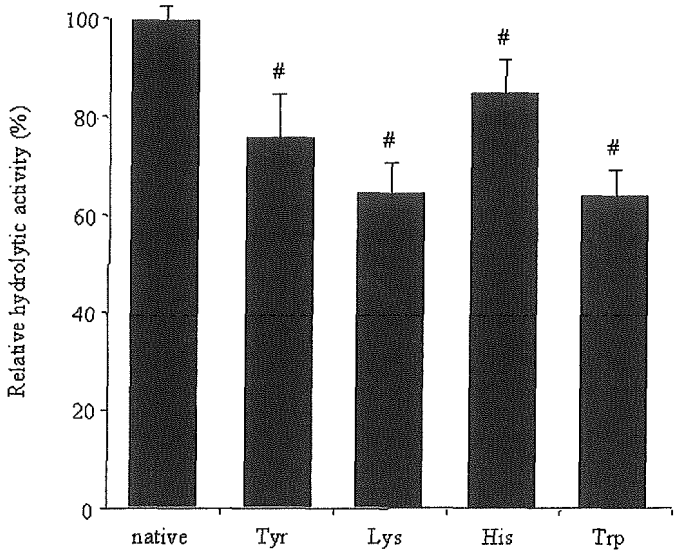

FIG. 4. Hydrolytic activities of chemically modified HSAs as compared with that of normal HSA. Reaction conditions: 75 μM HSA, 250 μM CS-866, 1/15 M phosphate buffer (pH 7.4), 37°C. Each column represents mean ± S.D. (n = 3). #, significantly different from native-type HSA ($p < 0.05$).

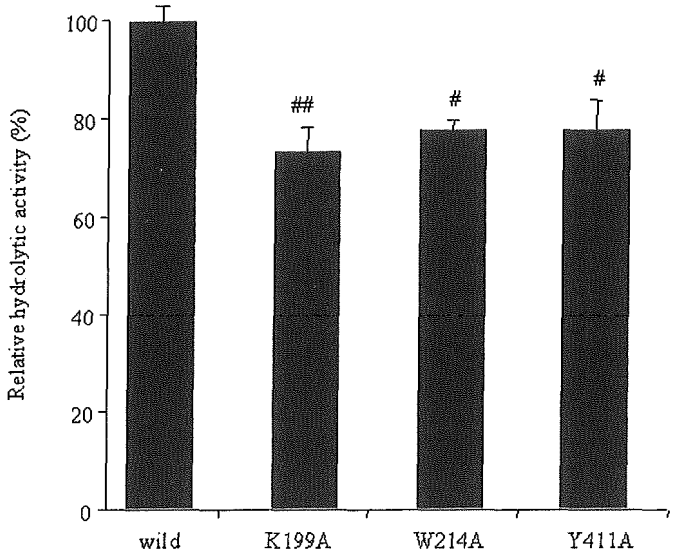

FIG. 5. Hydrolytic activities of mutant rHSAs as compared with that of wild-type rHSA. Reaction conditions: 75 μM HSA, 250 μM CS-866, 1/15 M phosphate buffer (pH 7.4), 37°C. Each column represents mean ± S.D. (n = 3). #, $p < 0.05$, and ##, $p < 0.01$ as compared with wild-type rHSA.

of the side chain of Glu-292 without steric hindrance as Glu-292 became capable of a nucleophilic reaction.

In model II, CS-866 was bound to site II using the pocket for myristate-4 (Fig. 7) (Curry et al., 1998). The pocket for myristate-3 was not occupied. The biphenyl moiety and the 2-propyl-imidazole moiety were bound to the hydrophobic pocket consisting of Leu-387, Pro-486 and Ala-490. The propan-2-ol moiety was surrounded by the hydrophobic residues (Leu-387, Leu-430, and Leu-453). Table 5 shows hydrogen bonds and electrostatic interactions in site II. Negative charges of the tetrazole moiety interacted electrostatically with the side chain of Arg-485, and the tetrazole moiety formed a hydrogen bond with the side chain of Asn-391. The side chain of Ser-489 formed hydrogen bonds with the hydroxyl oxygen atom of the propan-2-ol moiety and the carboxyl oxygen atom of the ester moiety. The carbonyl oxygen atom of the ester moiety formed a hydrogen bond with the side chain of Lys-414. The carboxyl oxygen atom of the ester moiety formed a hydrogen bond with the side chain of Tyr-411.

Discussion

This antihypertensive prodrug, CS-866, is hydrolyzed in the serum. Hydrolysis of CS-866 in serum has been observed in several species, and comparison among five species has shown that hydrolytic activity is highest in rabbits, followed by dogs, mice, rats, and humans (Ikeda, 2000). Furthermore, we examined the activity due to serum albumin. It was found to be highest in humans, followed by rats, mice, rabbits, and dogs (data not shown). This indicates that the mechanisms of hydrolysis of CS-866 in serum differ among those species, and that HSA plays a more important role in producing RNH-6270 than other serum albumin species.

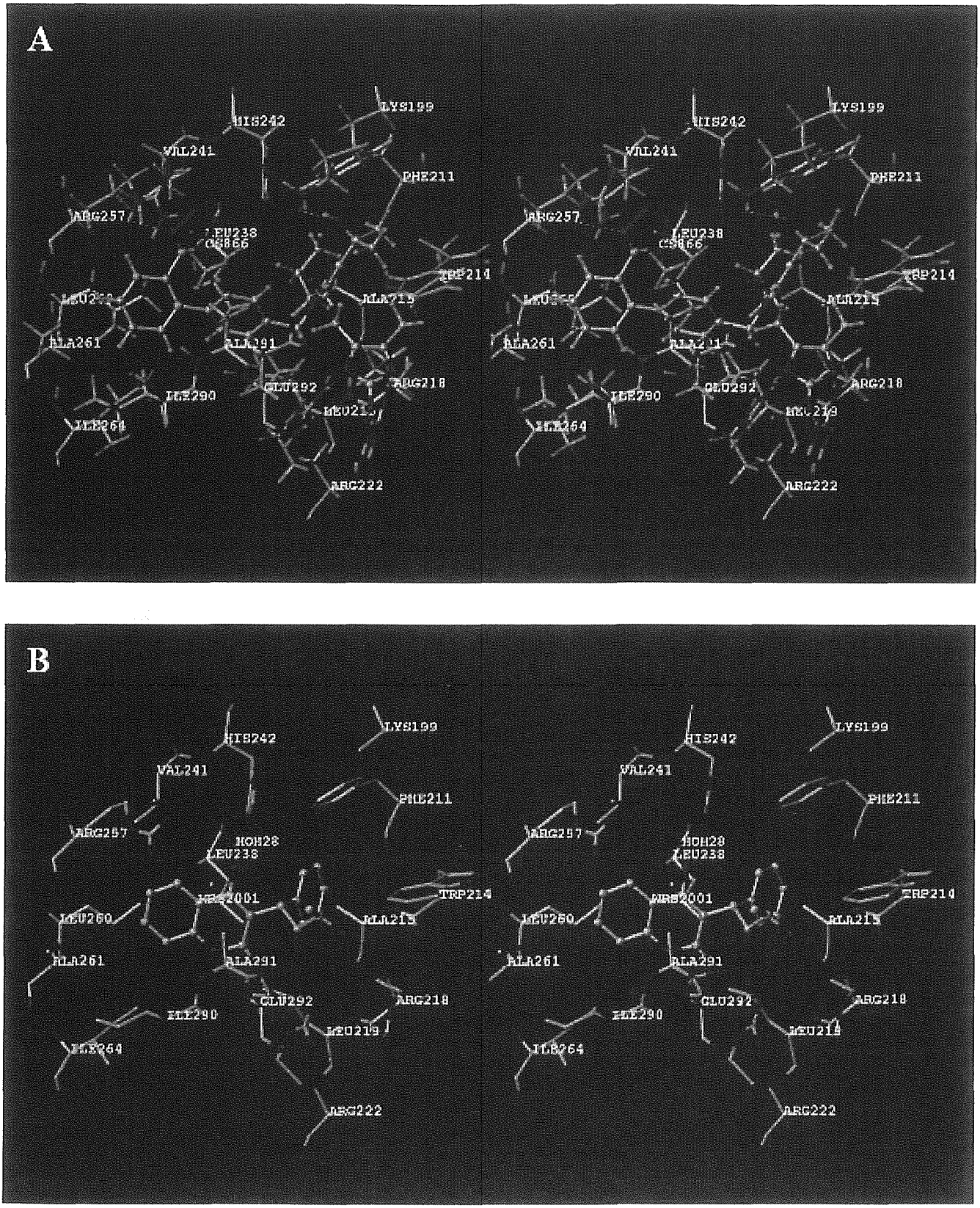

FIG. 6. Stereo drawings of ligands in site I. A, modeling structure for CS-866. The torsion angles of the side chain of Glu-292 were changed as Glu-292 becomes capable of a nucleophilic reaction. B, crystal structure for *S*-warfarin (PDB ID 1H9Z). Relaxed stereo viewing.

TABLE 4

Hydrogen bonds and electrostatic interactions in model I of HSA-CS-866 complex

Donor		Acceptor		Distance
				Å
Hydrogen bonds				
Lys-199	N_ζ	Ester	C=O	4.1
	N_ζ	Propan-2-ol	OH	3.0
Propan-2-ol	OH	His-242	Nϵ2	4.6
Arg-218	N_ϵ	Vinylene carbonate	O2	3.8
	N_η2		C=O	3.4
Arg-222	N_η2		C1	3.1
Positive		Negative		
Electrostatic interactions				
Lys-199	N_ζ	Tetrazole	N2	5.7
Arg-257	N_ϵ		N4	2.8

Thermodynamic Properties. The esterase-like activity of HSA is dependent on the catalytic rate constant, k_{cat}, and increases with a decrease in the activation free energy change, ΔG. Thus, the magnitude of ΔG, which is dependent on activation entropy change (ΔS), as calculated from a thermodynamic analysis, can be regarded as an indicator of hydrolytic activity of HSA (Fersht, 1998; Sakurai et al., 2004). Because PNPA has lower ΔG and ΔS values than CS-866 (Table 3), PNPA exhibited greater affinity for HSA and a higher catalytic rate than CS-866 (Table 2). Hydrolysis reactions catalyzed by albumin have previously been found to have a particularly great entropy difference between the ground state (ES) and the transition state (ES*) (Sakurai et al., 2004). The active sites of HSA to which the substrate binds are perfectly oriented to the reactive site of the substrate (the ester portion) for hydrolysis, and thus has a smaller entropy difference between the transition state (ES*) and the ground state (ES). This may be the reason why hydrolysis of PNPA proceeds more readily than hydrolysis of CS-866. That is, compared to CS-866, PNPA has a structure and orientation that are better suited to hydrolysis by HSA.

Relationship Between Ligand Binding Sites and Hydrolytic Active Sites. HSA is the most abundant protein in blood plasma and serves as a storage protein and transport protein for many endogenous and exogenous compounds (Peters, 1996; Kragh-Hansen et al., 2002). The unique capability of HSA to reversibly bind a large number of compounds is usually explained by the existence of a number of binding regions (including site I and site II), each of which has a very different specificity (Kragh-Hansen, 1991; Kragh-Hansen et al., 2002). Furthermore, site I on HSA consists of three subsites: Ia, Ib, and Ic (Fehske et al., 1982; Yamasaki et al., 1996). Another important role of HSA is as a catalyst for the hydrolysis of various compounds, such as esters, amides, and phosphates. It has been suggested that the active site of HSA for *p*-nitrophenyl esters is site II, and that Tyr-411 is essential for hydrolysis of *p*-nitrophenyl esters (Ozeki et al., 1980; Watanabe et al., 2000). The reactive site and active residue for nitroaspirin are reportedly site I and Lys-199, respectively (Ikeda and Kurono, 1986). The relationship between the hydrolytic active sites of HSA for CS-866 and the proteins' ligand-binding sites was investigated in the present study.

There are interesting patterns of competition between site I and site II ligands for hydrolysis. Although warfarin, which is regarded as a typical ligand of subsite Ia of HSA, acts as a competitive inhibitor, this does not necessarily indicate that the HSA catalytic site for CS-866 is subsite Ia, because ibuprofen, a typical site II ligand, also exhibited evidence of competitive inhibition (Figs. 2A and 3B). These results suggest that substrate specificity of the esterase-like region and ligand-binding site of HSA is inconsistent. In other words, the catalytic site for CS-866 on HSA may recognize CS-866 in a manner different from that of the ligand-binding site.

Roles of Specific Amino Acid Residues. For proteins whose X-ray crystallographic structure is known, the role of each amino acid residue can be quantitatively determined using the amino acid displacement (site-directed mutagenesis) technique and information obtained from X-ray analysis.

The present chemical modification experiments indicate that Lys, Trp, and Tyr residues of HSA are important for hydrolysis of CS-866 by HSA, and that His residues are also involved (Fig. 4). These experiments were performed with mildly modified HSA, because, for example, only 1.24 of the Tyr residues and 3.8 of the Lys residues were modified. However, HSA has 59 Lys residues, and the numbers of Trp, Tyr, and His residues are 1, 18, and 16, respectively. Previous findings have demonstrated that Tyr-411 is most likely the reactive Tyr of HSA (Watanabe et al., 2000). It is also known that the reactivity of Lys-199 is high (Means and Bender, 1975). Furthermore, it is reported that this single Trp residue contributes to the esterase-like activity of HSA (Ozeki et al., 1980; Kurono et al., 1982). In an attempt to identify specific residues of importance for the hydrolysis of CS-866, we examined the activity of several rHSAs, namely wild-type HSA and the single-residue mutants K199A, W214A, and Y411A.

Because we did not observe a great decrease of the hydrolytic activity of HSA for CS-866, even in the single-residue mutants K199A and Y411A, we conclude that the catalytic sites of HSA for CS-866 are not solely confined to the Lys-199 and Tyr-411 residues but, rather, involves several additional amino acid residues (Fig. 5).

The single Trp residue, Trp-214, is located close to Lys-199, as indicated by X-ray diffraction analysis, and is an element of a major interdomain cluster of hydrophobic residues (He and Carter, 1992; Sugio et al., 1999). The mutant W214A exhibited a significant decrease in hydrolytic activity (Fig. 5). In addition, the microenvironment near Trp-214 was investigated to obtain detailed information about the role of this residue in the hydrolysis. After incubation with CS-866 for 10 min, the relative fluorescence intensity of HSA decreased by more than half and the λ_{max} was blue-shifted (data not shown). These results are consistent with a model indicating that the Trp-214 residue is involved in hydrolytic reaction. These limited data lead us to the idea that a double (or triple) mutation of Lys-199, Trp-214, and Tyr-411 could completely abolish the hydrolytic activity. Further investigations on this point are under way at this laboratory.

Structural Mechanism of Hydrolysis Based on Models. The present findings suggest that HSA has two catalytic sites for CS-866, for the following two reasons. Mutation at site I or site II diminishes but does not abolish the hydrolytic activity. The hydrolytic activity is inhibited by both warfarin (site I drug) and ibuprofen (site II drug).

In model I (Fig. 6), CS-866 occupied the binding site of warfarin; this is consistent with the results showing that warfarin inhibits the hydrolytic activity of HSA. In site I, the carbonyl oxygen atom of the ester moiety formed a hydrogen bond with the side chain of Lys-199, and this hydrogen bond could function as an oxyanion hole. The importance of Lys-199 indicated by the model is consistent with the decreased hydrolytic activity of the K199A mutant and the HSA variant produced by chemical modification of Lys. The catalytic residue may be Glu-292; the distance between the oxygen atom of the side chain of Glu-292 and the carbonyl carbon of the ester moiety of CS-866 was 4.8 Å. The hydrophobic interaction between CS-866 and Trp-214 indicated by the model is consistent with the diminished

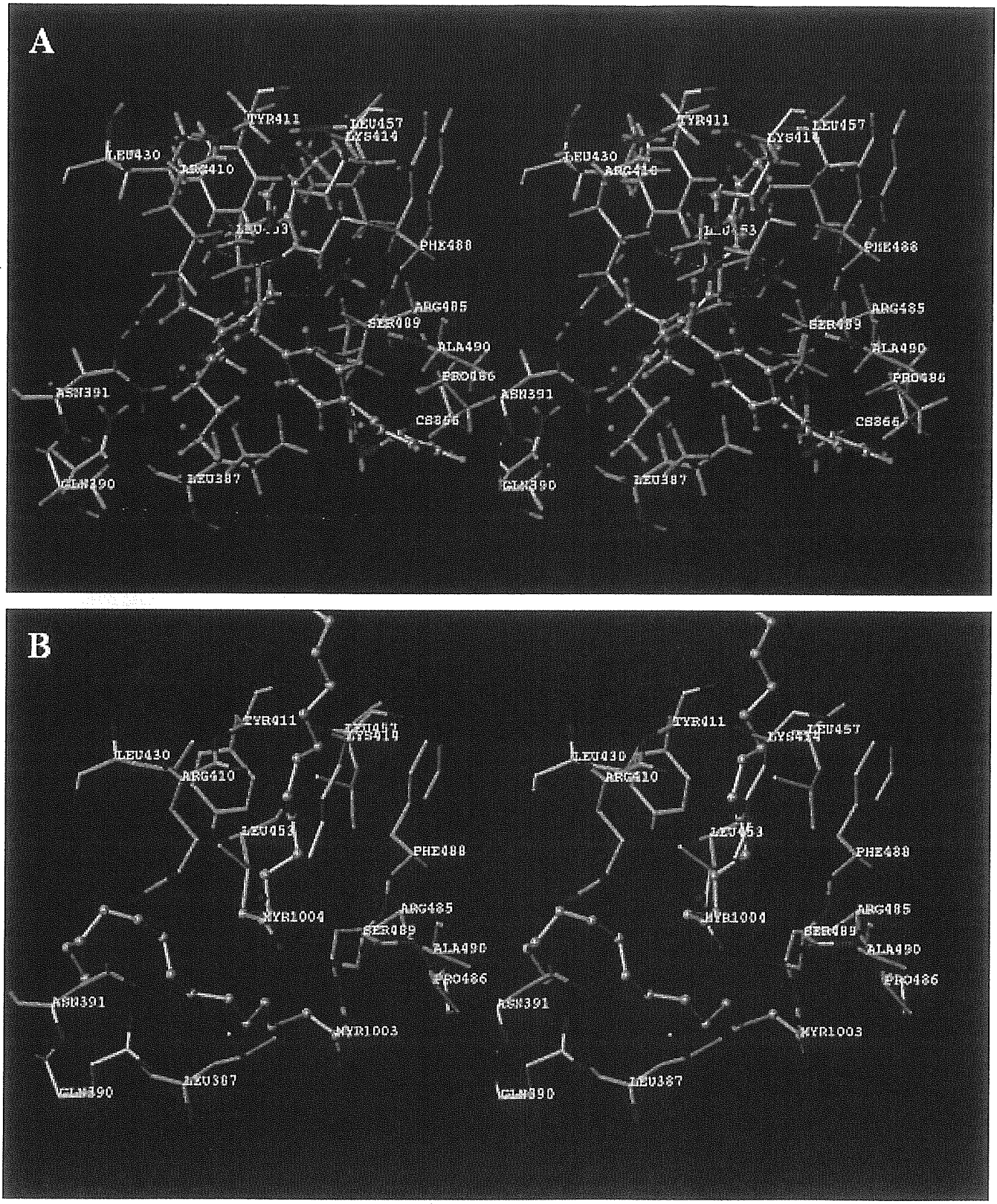

FIG. 7. Stereo drawings of ligands in site II. A, modeling structure for CS-866; B, crystal structure for myristate-3 and -4 (PDB ID 1H9Z). Relaxed stereo viewing.

hydrolytic activity of the W214A mutant and the HSA variant produced by chemical modification of Trp.

Model II (Fig. 7) indicates that the mechanism of hydrolysis of CS-866 is almost the same as that found in previous studies for *p*-nitrophenyl esters, with the exception of the involvement of Arg-410 (Watanabe et al., 2000; Sakurai et al., 2004). Instead of Arg-410, Lys-414 was used to create an oxyanion hole. The distance between the hydroxyl oxygen atom of Tyr-411 and the carbonyl carbon of the

TABLE 5

Hydrogen bonds and electrostatic interactions in model II of HSA-CS-866 complex

Donor		Acceptor		Distance
				Å
Hydrogen bonds				
Asn-391	$N_{\delta}2$	Tetrazole	N2	2.9
Tyr-411	O_{η}	Ester	–O–	2.8
Lys-414	N_{η}		C=O	2.7
Ser-489	O_{γ}		–O–	4.7
	O_{γ}	Propan-2-ol	OH	4.1
Positive		Negative		
Electrostatic interactions				
Arg-485	$N_{\eta}1$	Tetrazole	N3	3.5

ester moiety of CS-866 was 3.3 Å, indicating that it is possible that Tyr-411 plays the role of a cathartic residue. The importance of Tyr-411 and Lys-414 is consistent with the decreased hydrolytic activity of the Y411A mutant and of the HSA variants produced by chemical modification of Tyr or Lys. In our model II, CS-866 was bound to the pocket for myristate-4 in site II. The binding pockets of the site II ligands ibuprofen and diazepam are unknown. If ibuprofen binds to the pocket for myristate-4, our model II provides a mechanism for inhibition of hydrolytic activity of HSA by ibuprofen.

The present findings indicate that hydrolysis of CS-866 by HSA is dependent on ΔS. Another important factor is the orientation between the catalytic active site on HSA and the ester region of the substrate. There are differences between the catalytic active sites and the ligand-binding sites of HSA. Furthermore, the residues of Lys-199, Trp-214, and Tyr-411 play important roles in this catalytic reaction. All of these experimental findings are consistent with the docking model that we derived from computer simulation.

References

Brousil JA and Burke JM (2003) Olmesartan medoxomil: an angiotensin II-receptor blocker. *Clin Ther* **25**:1041–1055.

Chen RF (1967) Removal of fatty acids from serum albumin by charcoal treatment. *J Biol Chem* **242**:173–181.

Curry S, Mandelkow H, Brick P, and Franks N (1998) Crystal structure of human serum albumin complexed with fatty acid reveals an asymmetric distribution of binding sites. *Nat Struct Biol* **5**:827–835.

Cornell WD, Cieplak P, Bayly CI, Gould IR, Merz KM Jr, Ferguson DM, Spellmeyer DC, Fox T, Caldwell JW, and Kollman PA (1995) A second generation force field for the simulation of proteins, nucleic acids and organic molecules. *J Am Chem Soc* **117**:5179–5197.

Fehske KJ, Müller WE, and Wollert U (1978) The modification of the lone tryptophan residue in human serum albumin by 2-hydroxy-5-nitrobenzyl bromide. Characterization of the modified protein and the binding of L-tryptophan and benzodiazepines to the tryptophan-modified albumin. *Hoppe-Seylers Z Physiol Chem* **359**:709–717.

Fehske KJ, Schläfer U, Wollert U, and Müller WE (1982) Characterization of an important drug binding area on human serum albumin including the high-affinity binding sites of warfarin and azapropazone. *Mol Pharmacol* **21**:387–393.

Fersht A (1998) *Structure and Mechanism in Protein Science*, Freeman, New York.

Gasteiger J and Marsili M (1980) Iterative partial equalization of orbital electronegativity: a rapid access to atomic charges. *Tetrahedron* **36**:3219–3228.

Gasteiger J and Marsili M (1981) Prediction of proton magnetic resonance shifts: the dependence on hydrogen charges obtained by iterative partial equalization of orbital electronegativity. *Organ Magn Reson* **15**:353–360.

Gounaris AD and Perlmann GE (1967) Succinylation of pepsinogen. *J Biol Chem* **242**:2739–2745.

Haynes R, Osuga DT, and Feeney RE (1967) Modification of amino groups in inhibitors of proteolytic enzymes. *Biochemistry* **6**:541–547.

He XM and Carter DC (1992) Atomic structure and chemistry of human serum albumin. *Nature (Lond)* **358**:209–215.

Ikeda K and Kurono Y (1986) Enzymatic activity and drug binding activity of human serum albumin. *Yakugaku Zasshi* **106**:841–855.

Ikeda T (2000) Two prodrugs activated by serum esterases including albumin. Proceedings of the International Symposium on Serum Albumin & α_1-Acid Glycoprotein 173–180.

Koike H, Sada T, and Mizuno M (2001) In vitro and in vivo pharmacology of olmesartan medoxomil, an angiotensin II type AT1 receptor antagonist. *J Hypertens Suppl 19:* **1**:S3–S14.

Kragh-Hansen U (1991) Octanoate binding to the indole- and benzodiazepine-binding region of human serum albumin. *Biochem J* **273**:641–644.

Kragh-Hansen U, Chuang VTG, and Otagiri M (2002) Practical aspects of the ligand-binding and enzymatic properties of human serum albumin. *Biol Pharm Bull* **25**:695–704.

Kurono Y, Yamada H, and Ikeda K (1982) Effects of drug binding on the esterase-like activity of human serum albumin. V. Reactive site towards substituted aspirins. *Chem Pharm Bull* **30**:296–301.

Marsili M and Gasteiger J (1980) Pi-Charge Distributions from Molecular Topology and Pi-Orbital Electronegativity. *Croat Chem Acta* **53**:601–614.

Means GE and Bender ML (1975) Acetylation of human serum albumin by p-nitrophenyl acetate. *Biochemistry* **14**:4989–4994.

Neutel JM (2001) Clinical Studies of CS-866, the newest angiotensin II receptor antagonist. *Am J Cardiol* **87** (8A):37C–43C.

Ozeki Y, Kurono Y, Yotsuyanagi T, and Ikeda K (1980) Effects of drug binding on the esterase activity of human serum albumin: inhibition modes and binding sites of anionic drugs. *Chem Pharm Bull* **28**:535–540.

Peters T Jr (1996) *All about Albumin, Biochemistry, Genetics and Medical Applications*, Academic Press, San Diego.

Petitpas I, Bhattacharya AA, Twine S, East M, and Curry S (2001) Crystal structure analysis warfarin binding to human serum albumin: anatomy of drug site I. *J Biol Chem* **276**:22804–22809.

Purcel WP and Singer JA (1967) A brief review and table of semiempirical parameters used in the Hüeckel molecular orbital method. *J Chem Eng Data* **12**:235–246.

Rarey M, Kramer B, Lengauer T, and Klebe G (1996) A fast flexible docking method using incremental construction algorithm. *J Mol Biol* **261**:470–489.

Roosemont JL (1978) Reaction of histidine residues in proteins with diethylpyrocarbonate: differential molar absorptivities and reactivities. *Anal Biochem* **88**:314–320.

Sakurai Y, Ma SF, Watanabe H, Yamaotsu N, Hirono S, Kurono Y, Kragh-Hansen U, and Otagiri M (2004) Esterase-like activity of serum albumin: characterization of its structural chemistry using p-nitrophenyl esters as substrates. *Pharm Res (NY)* **21**:285–292.

Sokolovsky M, Riordan JF, and Vallee BL (1966) Tetranitromethane. A reagent for the nitration of tyrosyl residues in proteins. *Biochemistry* **5**:3582–3589.

Sugio S, Kashima A, Mochizuki S, Noda M, and Kobayashi K (1999) Crystal structure of human serum albumin at 2.5 A resolution. *Protein Eng* **12**:439–446.

Watanabe H, Tanase S, Nakajou K, Maruyama T, Kragh-Hansen U, and Otagiri M (2000) Role of Arg-410 and Tyr-411 in human serum albumin for ligand binding and esterase-like activity. *Biochem J* **349**:813–819.

Watanabe H, Yamasaki K, Kragh-Hansen U, Tanase S, Harada K, Suenaga A, and Otagiri M (2001) In vitro and in vivo properties of recombinant human serum albumin from Pichia pastoris purified by a method of short processing time. *Pharm Res (NY)* **18**:1775–1781.

Yamasaki K, Maruyama T, Kragh-Hansen U, and Otagiri M (1996) Characterization of site I on human serum albumin: concept about the structure of a drug binding site. *Biochim Biophys Acta* **1295**:147–157.

Address correspondence to: Professor Masaki Otagiri, Ph.D., Department of Biopharmaceutics, Graduate School of Pharmaceutical Sciences, Kumamoto University, 5-1 Oe-honmachi, Kumamoto 862-0973, Japan. E-mail: otagirim@gpo.kumamoto-u.ac.jp

doi:10.1016/j.jmb.2005.07.075 J. Mol. Biol. (2005) 353, 38–52

JMB

Available online at www.sciencedirect.com

SCIENCE DIRECT®

ELSEVIER

Structural Basis of the Drug-binding Specificity of Human Serum Albumin

Jamie Ghuman[1], Patricia A. Zunszain[1], Isabelle Petitpas[1] Ananyo A. Bhattacharya[1], Masaki Otagiri[2] and Stephen Curry[1]*

[1]*Biophysics Section, Division of Cell and Molecular Biology Imperial College London, South Kensington Campus, London SW7 2AZ, UK*

[2]*Faculty of Pharmaceutical Sciences, Kumamoto University 5-1 Oe-honmachi, Kumamoto 862-0973, Japan*

**Corresponding author*

Human serum albumin (HSA) is an abundant plasma protein that binds a remarkably wide range of drugs, thereby restricting their free, active concentrations. The problem of overcoming the binding affinity of lead compounds for HSA represents a major challenge in drug development. Crystallographic analysis of 17 different complexes of HSA with a wide variety of drugs and small-molecule toxins reveals the precise architecture of the two primary drug-binding sites on the protein, identifying residues that are key determinants of binding specificity and illuminating the capacity of both pockets for flexible accommodation. Numerous secondary binding sites for drugs distributed across the protein have also been identified. The binding of fatty acids, the primary physiological ligand for the protein, is shown to alter the polarity and increase the volume of drug site 1. These results clarify the interpretation of accumulated drug binding data and provide a valuable template for design efforts to modulate the interaction with HSA.

Keywords: human serum albumin; drug binding; drug specificity; protein crystallography

Introduction

Problems associated with adsorption, distribution, metabolism and elimination (ADME) add considerably to the complexity and cost of the development of new drugs[1] and are driving the search for techniques to optimise ADME characteristics at an early stage in the design process. One of the most important factors affecting the distribution and the free, active concentration of many administered drugs is binding affinity for human serum albumin (HSA). Albumin, the most abundant protein in human plasma (~600 μM), is a 66 kDa monomer containing three homologous helical domains (I–III), each divided into A and B subdomains (Figure 1(a)). The protein binds a wide variety of endogenous ligands including non-esterified fatty acids, bilirubin, hemin and thyroxine,[2] all of them acidic, lipophilic compounds, in multiple sites.[3–8] Many commonly used drugs with acidic or electronegative features (e.g. warfarin, diazepam, ibuprofen) also bind to HSA, usually at one of two primary sites (1 and 2), located in subdomains IIA and IIIA, respectively[9,10]. While a degree of albumin-binding may be desirable in helping to solubilize compounds that would otherwise aggregate and be poorly distributed, drugs with an excessively high affinity for the protein (> 95% bound) require correspondingly higher doses to achieve the effective concentration *in vivo*, can be slow to distribute to sites of action and may not be efficiently eliminated.[11–14]

Structural information on HSA–drug interactions has emerged only very recently and in a rather piecemeal fashion,[10,15–17] so most studies of drug binding have therefore adopted a ligand-based approach to the problem. For example, marker ligands for sites 1 and 2 have commonly been used in competition assays to identify the locus of binding of a range of different compounds.[9,18–20] More recently several pharmaceutical companies have developed high-throughput methods to assay the albumin-binding properties of their compound libraries.[13,21–25] The accumulated data can be used to develop quantitative structure–activity relationships for albumin binding.[12,14,26,27] However, the interpretation of competition or binding data is

Abbreviations used: HSA, human serum albumin; CMPF, 3-carboxy-4-methyl-5-propyl-2-furanpropanoic acid.

E-mail address of the corresponding author: s.curry@imperial.ac.uk

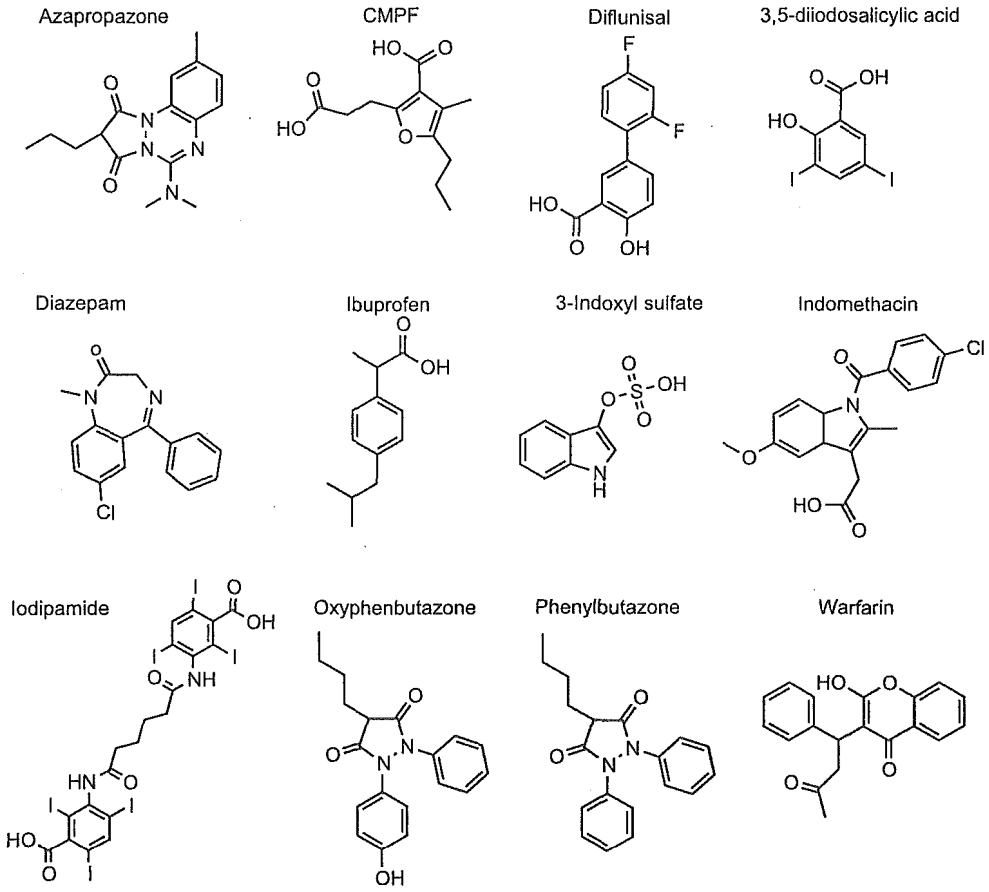

Figure 1. Chemical structures of the drug and toxin molecules used in this study.

non-trivial given the identification of partially overlapping binding compartments in site 1,[18–20] uncertainty as to the number of secondary drug-binding sites on the protein[20,28] and the possibility of allosteric interactions between drugs bound to sites 1 and 2.[29,30] Further complexities arise *in vivo* due to interactions between drugs and endogenous ligands for HSA.[31–33] This is particularly pertinent for fatty acids, which normally occur in serum at levels of between 0.1 and 2 mol per mol of HSA and can both compete and cooperate with drugs binding to the protein. In certain disease states, these effects are exacerbated as the fatty acid:HSA mole ratio may be as high as six.[34] Other pathological conditions are associated with high (micromolar to millimolar) levels of bilirubin, hemin or renal toxins (e.g. 3-carboxy-4-methyl-5-propyl-2-furanpropanoic acid (CMPF), indoxyl sulphate) which bind to the protein causing significant drug binding defects.[35–37]

Thus, although correlations based on large datasets of measurements of drug binding affinity have highlighted the importance of molecular descriptors such as lipophilicity, acidity, hydrogen bonding potential and shape factors in determining albumin binding,[13,27,38] such ligand-based approaches have yet to provide a wholly robust method for predicting the affinities of new compounds and structural information is clearly required to complement these investigations. We present here a crystallographic analysis of HSA complexed with a structurally diverse set of 12 drugs and small-molecule toxins (that are known to inhibit drug binding in renal patients), all of which bind to either site 1 or site 2[9,12,13,18,28,39,40] (Figure 1). We have also investigated the structural impact of drug–drug and drug–fatty acid interactions on the protein. The results provide new insights into the architecture and specificity of each drug pocket on HSA and reveal the molecular basis of the adaptability of this versatile transporter protein.

Results and Discussion

Structure determination and overview

HSA–drug and HSA-myristate–drug complexes were prepared either by co-crystallisation or crystal-soaking using relatively high (millimolar) drug concentrations, to help overcome the effect of the presence of ~30% (v/v) polyethlyene glycol in the crystal and thereby ensure good occupancy (Materials and Methods; Supplementary Data). The

structures of the drug complexes were solved by molecular replacement using previously determined structures of HSA[16] or HSA-myristate[4] as appropriate, since there were no gross conformational changes associated with drug binding. The shape of the difference electron density, coupled with consideration of the chemical nature of the binding environment, generally gave an unambiguous indication of the bound drug conformation (Figure 2). In a few cases, particularly complexes that were determined at lower resolutions (~3 Å), refinement of alternative drug orientations was used to determine the most plausible conformation. Models for the various complexes were refined to resolutions of 2.25–3.20 Å and have R_{free} values in the range 24.3–29.2% and good stereochemistry (Table 1).

Drug site 1 in defatted HSA

Drug site 1 is a pre-formed binding pocket within the core of subdomain IIA that comprises all six helices of the subdomain and a loop-helix feature (residues 148–154) contributed by IB. The interior of the pocket is predominantly apolar but contains two clusters of polar residues, an inner one towards the bottom of the pocket (Y150, H242, R257) and an outer cluster at the pocket entrance (K195, K199, R218, R222) (Figure 3). The large binding cavity is comprised of a central zone from which extend three distinct compartments. The back end of the pocket is divided by I264 into left and right hydrophobic sub-chambers (according to the viewpoint in Figure 3(a)–(c)), whereas a third sub-chamber protrudes from the front of the pocket, delineated by F211, W214, A215, L238 and aliphatic portions of K199 and R218.

As expected, CMPF, oxyphenbutazone, phenylbutazone and warfarin cluster in the centre of the site 1 pocket. In site 1 the ligands invariably have a planar group pinned snugly between the apolar side-chains of L238 and A291; in contrast there is much greater variation in the drug position within the plane perpendicular to the line between these two residues. This is particularly evident at the mouth of the pocket where the wide opening and

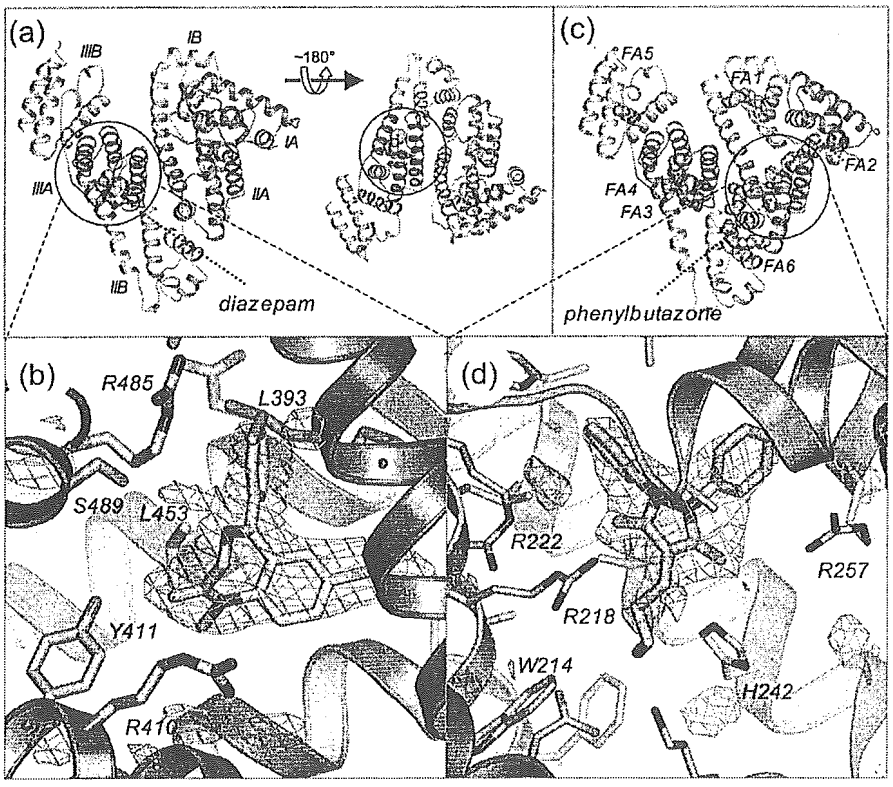

Figure 2. Overview of HSA structure and omit maps. (a) Structure of HSA–diazepam. The protein is colour-coded by subdomain using a scheme that is maintained throughout. The diazepam is depicted in space-filling representation colour-coded by atom-type: carbon, pink; oxygen, red; nitrogen, blue; chlorine, gr. The rotated view on the right shows drug site 2 in the same orientation as drug site 1 in (c). (b) F_o-F_c simulated annealing omit map calculated in CNS[50] with the diazepam molecule omitted from the phasing model and contoured at 2.75σ. (c) Structure of HSA-myristate-phenylbutazone. Fatty acid molecules and phenylbutazone are depicted in space-filling representation with carbon atoms coloured grey and mid-blue, respectively. (d) F_o-F_c simulated annealing omit map calculated with the phenylbutazone molecule omitted from the phasing model and contoured at 2.75σ. All Figures were prepared using PyMol.[55]

Table 1. Data collection and refinement statistics

Drug site	Myr[a]	Drug[b]	SG[c]	Resolution (Å)	N_{ref}[d]	R_{merge} (%)[e]	I/σ_I[f]	Multiplicity	Completeness (%)	N_{atoms}[g]	R_{work} (%)	R_{free} (%)	B_{av} (Å^2)	rms_{bonds} (Å)	rms_{angles} (Å)	PDB ID
1	−	aza	*P*1	41.4–2.70	32,322	4.1 (30.5)	12.2 (2.9)	2.0 (2.0)	95.6 (95.4)	8669	23.6	27.4	77.9	0.009	1.42	2bx8
1	−	cmpf	*P*1	49.2–2.35	50,096	3.6 (37.6)	10.3 (2.2)	1.8 (1.7)	95.5 (95.2)	8664	23.1	26.1	68.6	0.007	1.20	2bxa
1	−	oxy	*P*1	22.9–3.20	22,484	7.2 (34.2)	8.0 (2.5)	1.8 (1.8)	96.8 (97.0)	8790	22.8	27.6	71.0	0.006	1.23	2bxb
1	−	pbz	*P*1	36.4–3.10	22,396	10.5 (35.0)	7.0 (2.0)	2.0 (2.0)	98.4 (98.4)	8804	25.2	29.2	72.7	0.005	1.02	2bxc
1	−	wrf	*P*1	49.3–3.05	23,406	6.0 (36.9)	8.9 (2.3)	1.9 (1.9)	97.7 (97.0)	8632	21.3	26.0	73.2	0.008	1.29	2bxd
1	+	aza	*C*2	34.4–2.45	24,928	5.4 (38.1)	10.9 (3.2)	2.5 (2.5)	99.3 (99.9)	4633	20.8	26.5	54.5	0.007	1.21	2bxi
1	+	aza-imn	*C*2	22.3–2.40	25,123	4.1 (32.2)	13.6 (3.6)	2.6 (2.5)	95.1 (95.1)	4648	20.9	25.3	49.8	0.007	1.21	2bxk
1	+	dis	*C*2	12.8–2.60	17,736	5.2 (19.8)	12.4 (4.4)	2.4 (2.3)	83.9 (87.2)	4565	20.0	24.3	59.9	0.007	1.21	2bxl
1	+	imn	*C*2	34.5–2.5	23,052	5.7 (38.7)	8.4 (2.1)	1.7 (1.7)	97.8 (97.8)	4665	20.1	24.8	57.5	0.007	1.24	2bxm
1	+	iod	*C*2	34.5–2.65	19,370	5.4 (37.6)	11.4 (3.0)	2.7 (2.7)	97.8 (99.6)	4671	20.8	26.5	56.7	0.007	1.26	2bxn
1	+	oxy	*C*2	38.0–2.60	20,377	6.0 (40.0)	10.9 (2.9)	2.9 (2.9)	96.9 (98.4)	4648	19.5	25.3	58.8	0.007	1.26	2bxo
1	+	pbz	*C*2	34.4–2.30	28,916	6.1 (31.1)	10.0 (2.7)	2.1 (2.1)	96.8 (97.8)	4651	21.1	25.0	51.3	0.006	1.18	2bxp
1	+	pbz-imn	*C*2	22.3–2.60	20,764	5.4 (36.3)	13.1 (3.5)	3.0 (3.0)	98.6 (99.4)	4658	19.5	25.7	52.0	0.007	1.24	2bxq
2	−	dfl	*P*1	38.2–2.95	26,848	5.0 (32.5)	9.4 (2.4)	2.0 (2.0)	98.4 (98.2)	8710	22.6	27.0	82.0	0.009	1.32	2bxe
2	−	dzp	*P*1	22.6–2.90	27,722	4.8 (36.1)	10.8 (2.6)	1.9 (1.9)	96.6 (96.8)	8615	21.5	26.2	81.5	0.007	1.25	2bxf
2	−	ibu	*P*1	22.4–2.70	33,880	4.6 (32.1)	11.2 (2.8)	2.0 (1.9)	96.8 (96.6)	8773	23.4	28.2	75.0	0.007	1.22	2bxg
2	−	ids	*P*1	36.3–2.25	58,748	3.9 (38.6)	10.7 (2.5)	2.0 (2.0)	98.7 (98.1)	8625	22.7	26.6	69.3	0.009	1.32	2bxh

[a] Indicates presence or absence of myristate in the HSA–drug complex.
[b] Abbreviated names for drugs used here and in Figures are: aza, azapropazone; cmpf, 3-carboxy-4-methyl-5-propyl-2-furanpropanoic acid; dfl, diflunisal; dis, diiodosalicylic acid; dzp, diazepam; ibu, ibuprofen; ids, indoxyl sulfate; imn, indomethacin; iod, iodipamide; oxy, oxyphenbutazone; pbz, phenylbutazone; rwf, *R*(+)-warfarin.
[c] Space group.
[d] Number of independent reflections.
[e] Figures in parentheses indicate values for highest-resolution shell.
[f] Signal to noise ratio output from SCALA.
[g] Total number of atoms in the refined model.